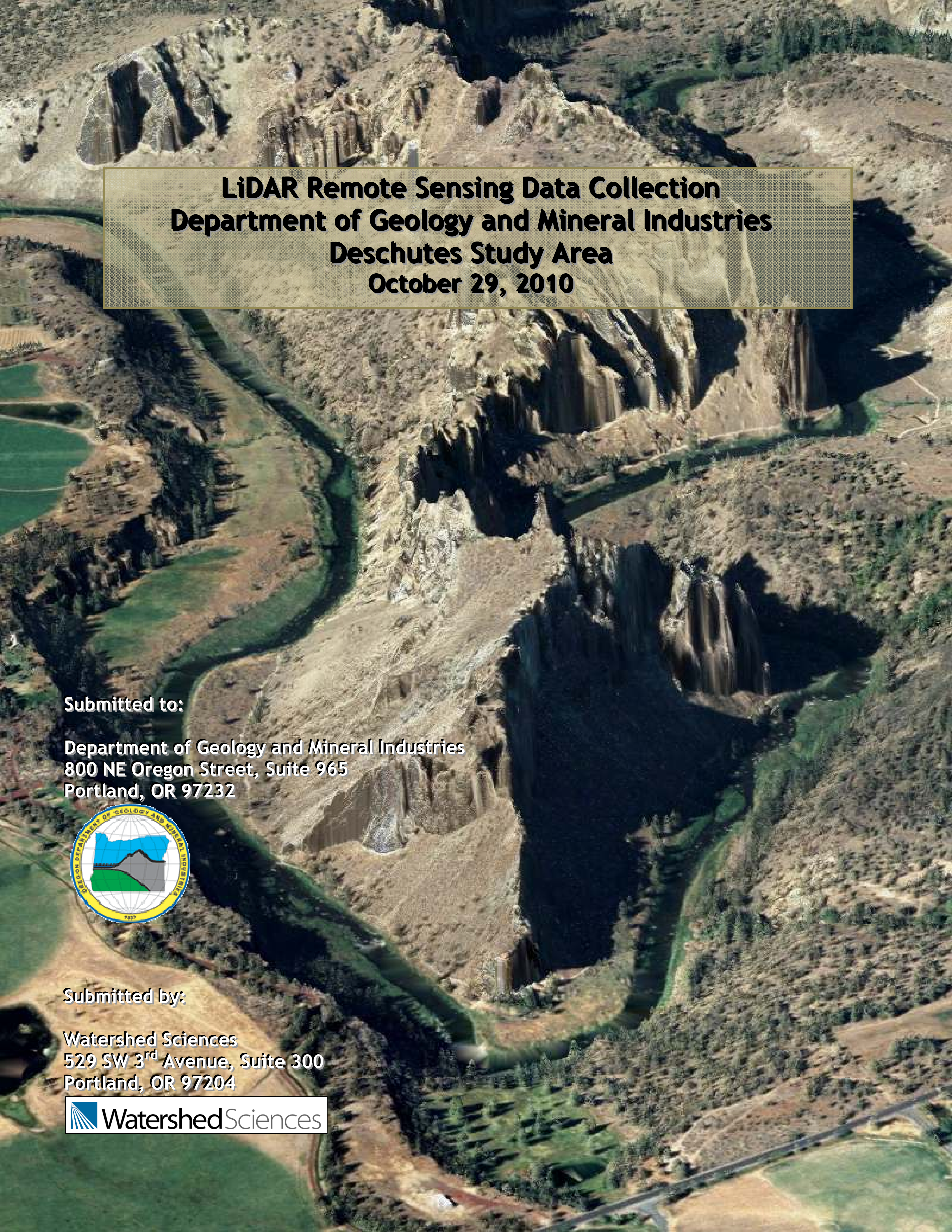

LiDAR Remote Sensing Data Collection
Department of Geology and Mineral Industries
Deschutes Study Area
October 29, 2010

Submitted to:

Department of Geology and Mineral Industries
800 NE Oregon Street, Suite 965
Portland, OR 97232

Submitted by:

Watershed Sciences
529 SW 3rd Avenue, Suite 300
Portland, OR 97204

LiDAR Remote Sensing Data Collection:
DOGAMI, Deschutes Study Area

TABLE OF CONTENTS

1. Overview

1.1 Study Area

Watershed Sciences, Inc. has collected Light Detection and Ranging (LiDAR) data of the Deschutes Study Area for the Oregon Department of Geology and Mineral Industries (DOGAMI). The area of interest (AOI) totals 2,899 square miles (1,855,419 acres) and the total area flown (TAF) covers 2,950 square miles (1,888,159 acres). The TAF acreage is greater than the original AOI acreage due to buffering and flight planning optimization (**Figure 1.1** below). The DOGAMI study area will be acquired and processed as logistical constraints and weather allow. This report will be amended to reflect new data and cumulative statistics for the overall LiDAR survey with every delivery. DOGAMI data are delivered in OGIC (HARN): Projection: Oregon Statewide Lambert Conformal Conic; horizontal and vertical datum: NAD83 (HARN)/NAVD88 (Geoid03); units: International Feet.

Figure 1.1. *DOGAMI Deschutes Study Area.*

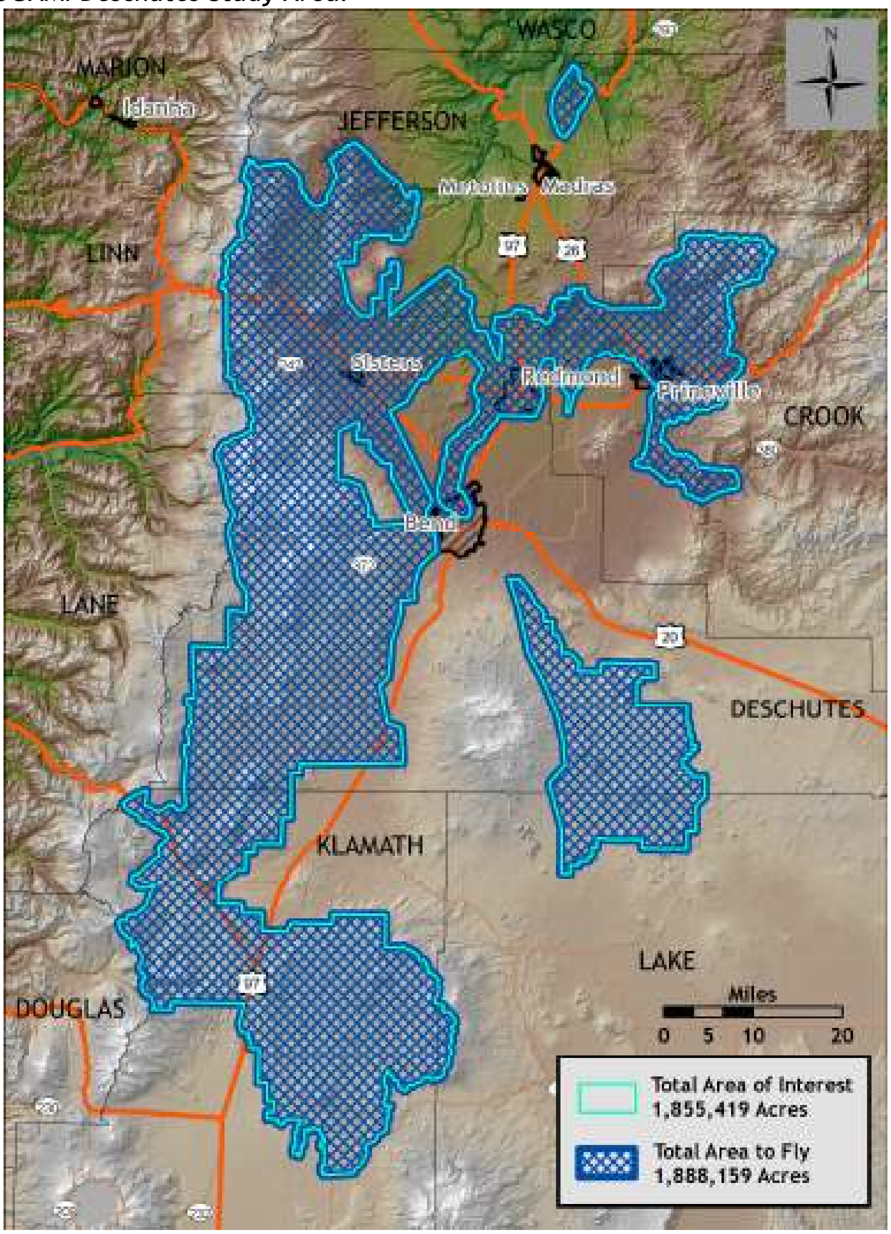

1.2 Area Delivered to Date

Total delivered acreage to date is detailed below and in **Figure 1.2**.

DOGAMI Deschutes Study Area				
	Delivery Date	**Acquisition Dates**	**AOI Acres**	**TAF Acres**
Delivery Area 1	January 5, 2010	Oct. 2, 2009	12,728	13,507
Delivery Area 2	February 26, 2010	Oct. 5 - 11, 2009	76,802	78,268
Delivery Area 3	March 5, 2010	Oct. 11-17, 2009	111,024	113,101
Delivery Area 4	April 9, 2010	Oct. 7 – 11, 2009	163,085	163,814
Delivery Area 5	March 5, 2010	Oct. 1-12, 2009	78,541	80,720
Delivery Area 6	March 12, 2010	Oct. 17-23, 2009	54,655	55,470
Delivery Area 7	March 23, 2010	Oct. 18-20; Nov 1-4 2009	150,101	151,426
Delivery Area 8	April 16, 2010	Oct. 8-23, 2009	100,266	102,343
Delivery Area 9	September 3, 2010	Oct. 11-16, 2009; June 14, 2010	30,144	31,969
Delivery Area 10	September 3, 2010	Oct. 12-17, 2009 May 29-June 17, 2010	48,721	50,833
Delivery Area 11	September 22, 2010	Oct. 16-Nov 5, 2009 May 28 - July 3, 2010	229,028	231,807
Delivery Area 12	October 29, 2010	Oct. 16-Nov 5, 2009 May 28 - July 3, 2010	169,744	172,978
Total Acres Delivered			**1,224,839**	**1,246,236**

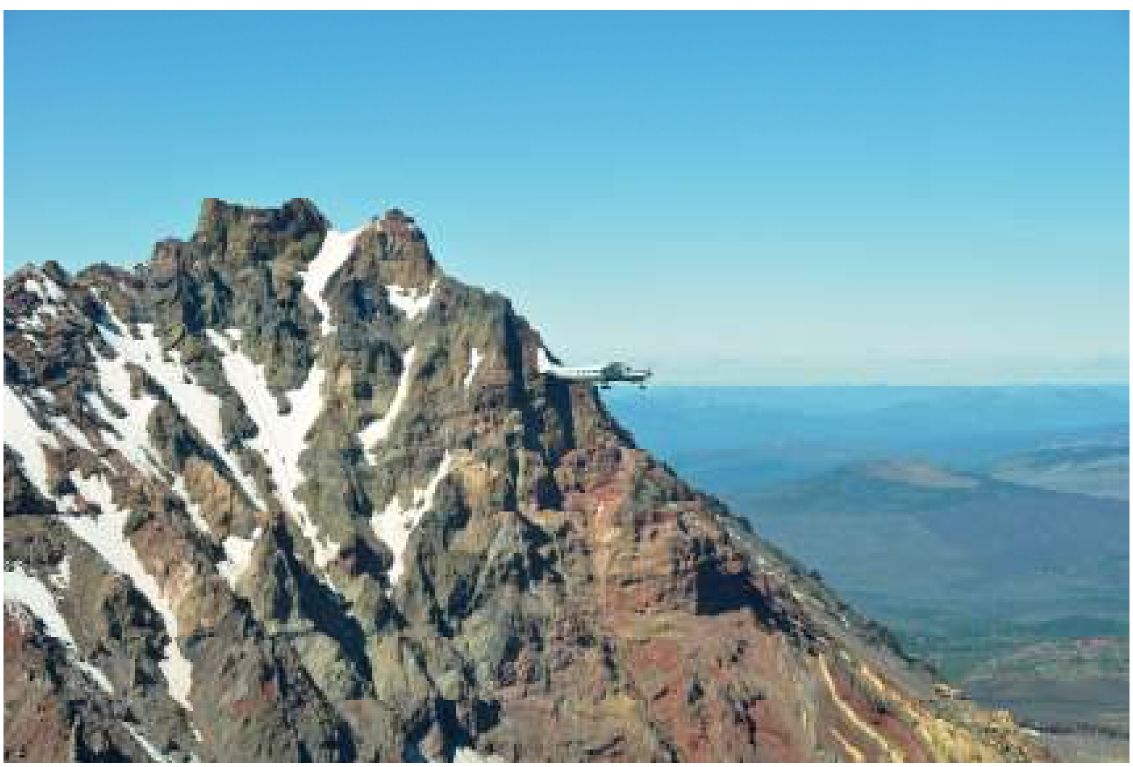

***Figure 1.2**. Deschutes Study Area, illustrating the delivered portions of the TAF.*

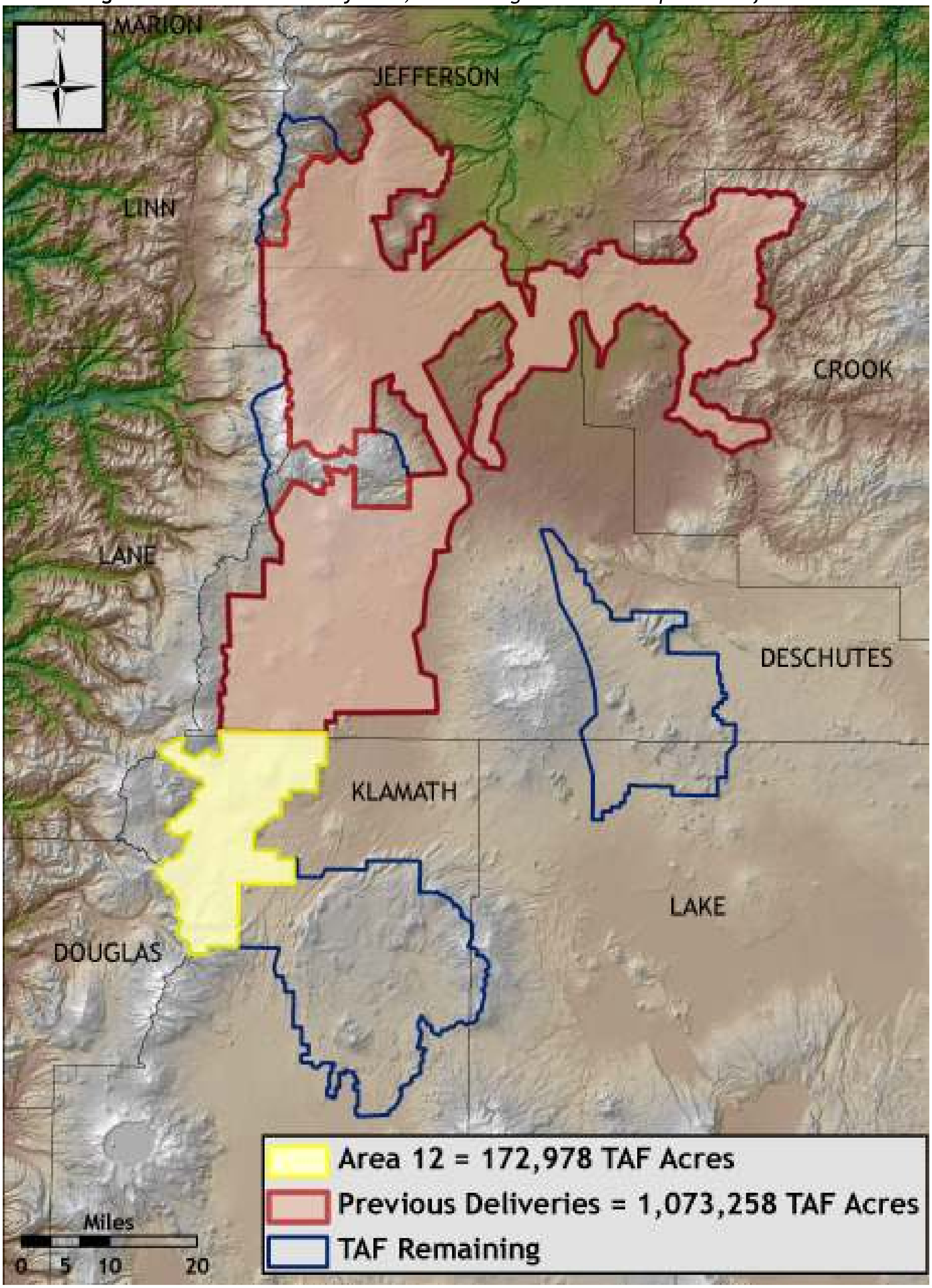

Figure 1.3. Deschutes Study Area, illustrating the delivered 7.5 minute USGS quads.

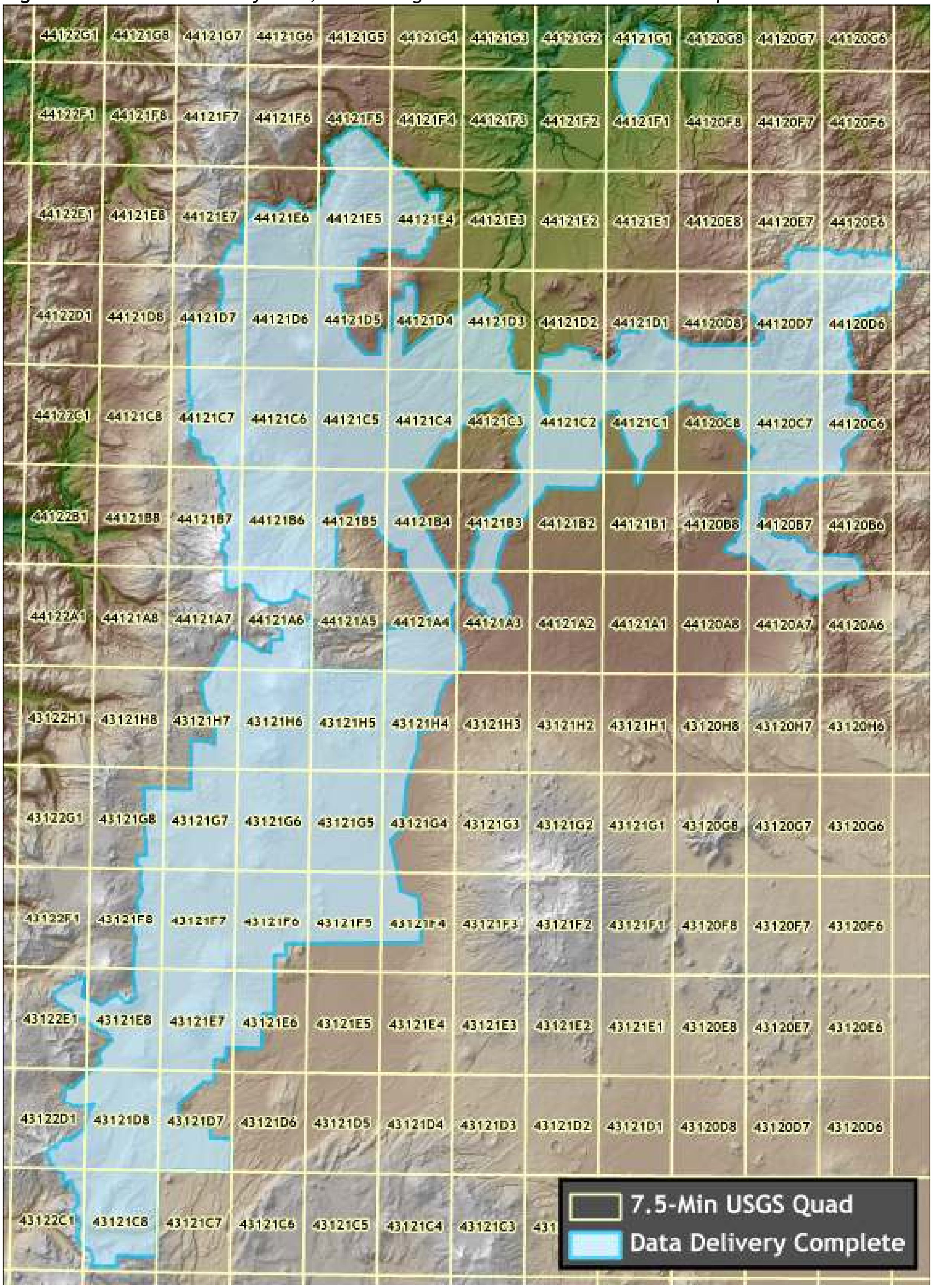

2. Acquisition

2.1 Airborne Survey Overview – Instrumentation and Methods

The LiDAR survey utilized Leica ALS50 Phase II and ALS60 sensors mounted in multiple Cessna Caravan 208Bs. The Leica systems was set to acquire ≥105,000 laser pulses per second (i.e. 105 kHz pulse rate) and flown at 900 and 1300 meters above ground level (AGL), capturing a scan angle of ±14° from nadir[1]. These settings are developed to yield points with an average native density of ≥8 points per square meter over terrestrial surfaces. The native pulse density is the number of pulses emitted by the LiDAR system. Some types of surfaces (i.e. dense vegetation or water) may return fewer pulses than the laser originally emitted. Therefore, the delivered density can be less than the native density and lightly variable according to distributions of terrain, land cover and water bodies.

The Cessna Caravan is a powerful, stable platform, which is ideal for the often remote and mountainous terrain found in the Pacific Northwest. The Leica ALS60 sensor head installed in the Caravan is shown on the right.

Table 2.1 *LiDAR Survey Specifications*

Sensors	Leica ALS50 Phase II and ALS60
Survey Altitudes (AGL)	900 m and 1300 m
Pulse Rate	>105 kHz
Pulse Mode	Single
Mirror Scan Rate	52 Hz
Field of View	28° (±14° from nadir)
Roll Compensated	Up to 15°
Overlap	100% (50% Side-lap)

The study area was surveyed with opposing flight line side-lap of ≥50% (≥100% overlap) to reduce laser shadowing and increase surface laser painting. The system allows up to four range measurements per pulse, and all discernable laser returns were processed for the output dataset.

To solve for laser point position, it is vital to have an accurate description of aircraft position and attitude. Aircraft position is described as x, y and z and measured twice per second (2 Hz) by an onboard differential GPS unit. Aircraft attitude is measured 200 times per second (200 Hz) as pitch, roll and yaw (heading) from an onboard inertial measurement unit (IMU). **Figure 2.1** shows the flight lines completed for the area delivered to date.

[1] Nadir refers to the perpendicular vector to the ground directly below the aircraft. Nadir is commonly used to measure the angle from the vector and is referred to a “degrees from nadir”.

Figure 2.1. *Actual flightlines for the Deschutes Study Area illustrating the dates flown (based on GPS week) for current deliveries.*

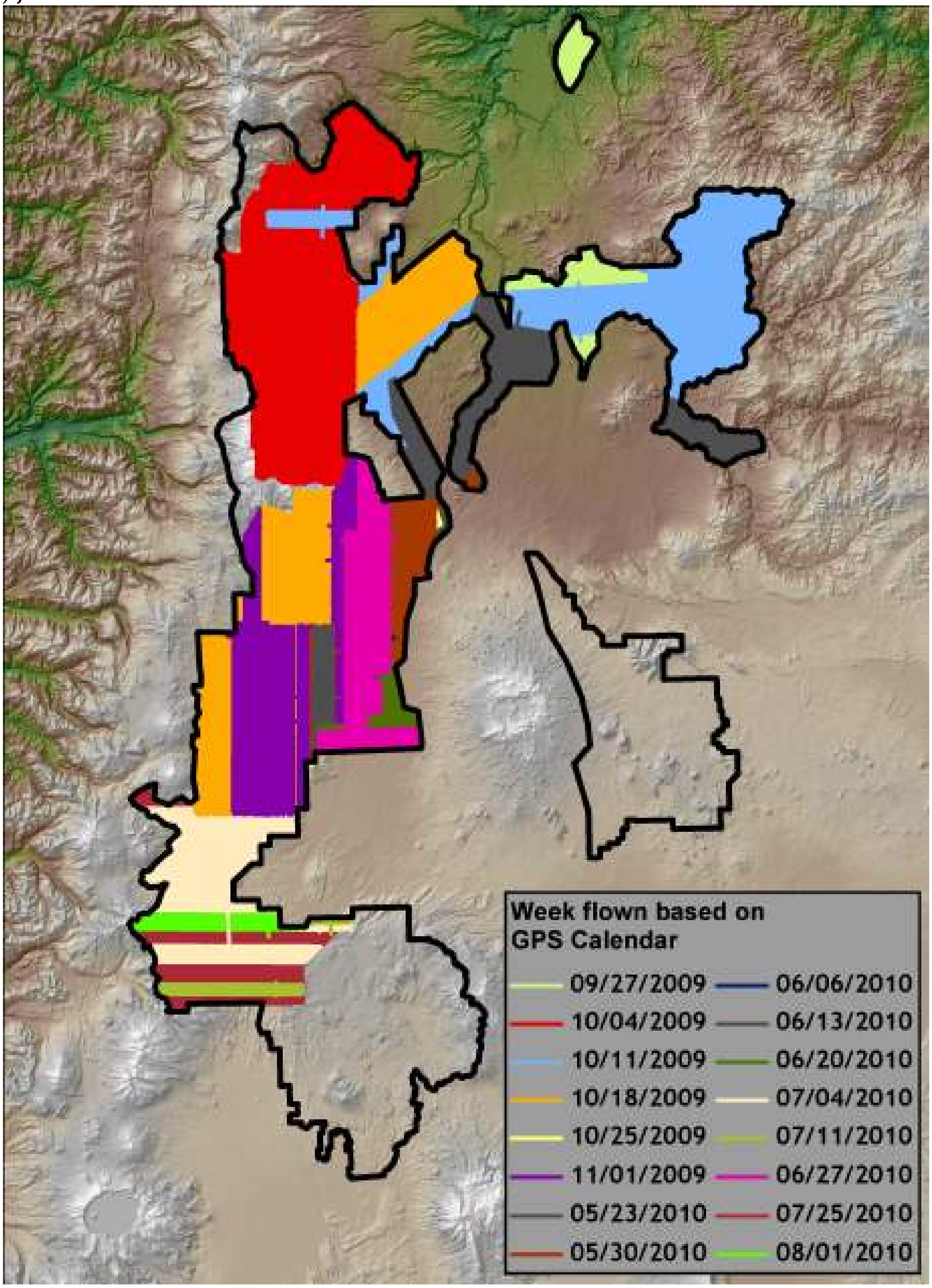

2.2 Ground Survey – Instrumentation and Methods

During the LiDAR survey, static (1 Hz recording frequency) ground surveys were conducted over either known or set monuments. Monument coordinates are provided in **Table 2.2** and shown in **Figure 2.2** for the AOI. After the airborne survey, the static GPS data are processed using triangulation with continuous operation stations (CORS) and checked using the Online Positioning User Service (OPUS[2]) to quantify daily variance. Multiple sessions are processed over the same monument to confirm antenna height measurements and reported position accuracy.

2.2.1 Instrumentation

For this delivery area all Global Navigation Satellite System (GNSS[3]) survey work uses a Trimble GPS receiver model R7 with a Zephyr Geodetic antenna and ground plane for static control points. A Trimble GPS R8 unit is used primarily for RTK work but when needed it can be used as a static receiver as well. For RTK data, the collector begins recording after remaining stationary for 5 seconds then calculating the pseudo range position from at least three epochs with the relative error under 1.5cm horizontal and 2cm vertical. All GPS measurements are made with dual frequency L1-L2 receivers with carrier-phase correction.

2.2.2 Monumentation

Whenever possible, existing and established survey benchmarks shall serve as control points during LiDAR acquisition including those previously set by Watershed Sciences. In addition to NGS, the county surveyor's offices and ODOT often establish their own benchmarks. NGS benchmarks are preferred for control points. In the absence of NGS benchmarks, county surveys, or ODOT monumentation, Watershed Sciences produces our own monuments. These monuments are spaced at a minimum of one mile and every effort is made to keep these monuments within the public right of way. If monuments are required on private property, consent from the owner is required. All monumentation is done with 5/8" x 24" or 30" rebar topped with an orange plastic cap (prior to January, 2010) and with an aluminum cap (from January 2010 to present).

[2] Online Positioning User Service (OPUS) is run by the National Geodetic Survey to process corrected monument positions.
[3] GNSS: Global Navigation Satellite System consisting of the U.S. GPS constellation and Soviet GLONASS constellation

2.2.3 Methodology

Each aircraft is assigned a ground crew member with two R7 receivers and an R8 receiver. The ground crew vehicles are equiped with standard field survey supplies and equipment including safety materials. All data points are observed for a minimum of two survey sessions lasting no fewer than 6 hours. At the beginning of every session the tripod and antenna are reset, resulting in two independent instrument heights and data files. Data are collected at a rate of 1Hz using a 10 degree mask on the antenna.

The ground crew uploads the GPS data to the FTP site on a daily basis to be returned to the office for PLS oversight, QA/QC review and processing. OPUS processing triangulates the monument position using 3 CORS stations resulting in a fully adjusted position. CORPSCON[4] 6.0.1 software is used to convert the geodetic positions from the OPUS reports. After multiple days of data have been collected at each monument, accuracy and error ellipses are calculated. This information leads to a rating of the monument based on FGDC-STD-007.2-1998[5] Part 2 table 2.1 at the 95% confidence level.

All GPS measurements are made during periods with PDOP less than or equal to 3.0 and with at least 6 satellites in view of both a stationary reference receiver and the roving receiver. RTK positions are collected on 20% of the flight lines and on bare earth locations such as paved, gravel or stable dirt roads, and other locations where the ground is clearly visible (and is likely to remain visible) from the sky during the data acquisition and RTK measurement period(s). In order to facilitate comparisons with LiDAR measurements, RTK measurements are not taken on highly reflective surfaces such as center line stripes or lane markings on roads. In addition, it is desirable to include locations that can be readily identified and occupied during subsequent field visits in support of other quality control procedures described later. Examples of identifiable locations would include manhole and other flat utility structures that have clearly indicated center points or other measurement locations. In the absence of utility structures, a PK nail can be driven into asphalt or concrete and marked with paint.

[4] U.S. Army Corps of Engineers , Engineer Research and Development Center Topographic Engineering Center software
[5] Federal Geographic Data Committee Draft Geospatial Positioning Accuracy Standards

__Figure 2.2__. Base stations for the Deschutes Study Area for data delivered to date.

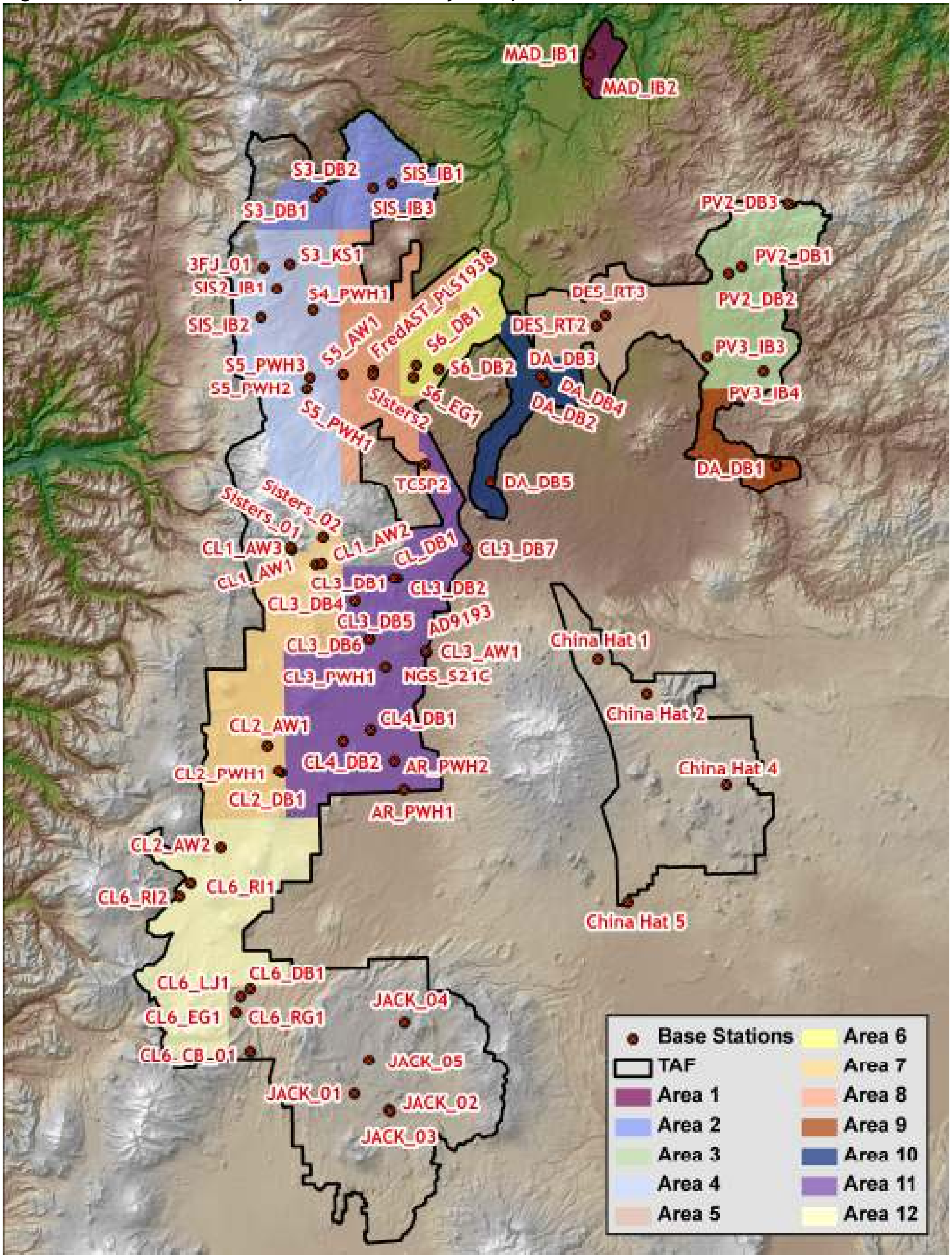

Table 2.2. *Base Station Surveyed Coordinates, (NAD83/NAVD88, OPUS corrected) used for kinematic post-processing of the aircraft GPS data for the Deschutes Study Area in **2009**.*

	Datum NAD83 (HARN)		GRS80
Base Stations ID	**Latitude (North)**	**Longitude (West)**	**Ellipsoid Height (m)**
CL1_AW1	44 00 11.68842	121 40 50.12824	1914.182
CL1_AW2	44 00 16.69262	121 40 04.34254	1899.735
CL1_AW3	44 01 31.45566	121 43 48.33634	1637.650
CL2_AW1	43 44 01.10212	121 47 08.62177	1298.569
CL2_AW2	43 35 1.53931	121 53 3.72446	1334.811
CL2_DB1	43 41 36.78416	121 45 29.96714	1300.030
CL2_PWH1	43 41 47.61505	121 45 49.78708	1300.985
CL3_DB1	43 58 48.63125	121 31 14.42329	1602.125
DES_RT2	44 20 56.78639	121 05 28.44007	847.267
DES_RT3	44 21 48.46263	121 04 21.28445	839.760
FredAST_PLS1938	44 17 25.33409	121 33 18.25920	953.378
MAD_IB1	44 45 17.99134	121 05 30.55012	638.251
MAD_IB2	44 42 43.10030	121 05 50.80549	641.072
PV2_DB1	44 25 57.61697	120 47 13.34425	986.631
PV2_DB2	44 25 24.97372	120 48 51.76166	967.022
PV2_DB3	44 31 21.94274	120 41 10.80400	1537.742
PV3_IB3	44 18 00.14713	120 51 50.79538	953.144
S3_DB1	44 32 53.93542	121 40 09.12051	948.395
S3_DB2	44 33 28.00859	121 39 20.60152	937.014
S3_KS1	44 27 02.22135	121 43 29.33220	990.974
S4_PWH1	44 22 52.59100	121 40 41.21292	1005.952
S5_AW1	44 17 11.13065	121 37 05.09836	1009.735
S5_PWH1	44 15 50.54444	121 41 36.40461	1277.950
S5_PWH2	44 15 52.54934	121 41 36.18206	1274.839
S5_PWH3	44 16 55.30769	121 41 11.96243	1184.015
S6_DB1	44 17 50.87280	121 27 57.61082	923.456
S6_DB2	44 17 26.98022	121 25 12.17361	909.928
S6_EG1	44 16 48.49596	121 28 22.62132	928.845
SIS_IB1	44 34 09.04366	121 30 37.46176	1083.141
SIS_IB2	44 22 17.16094	121 47 11.84116	1512.582
SIS_IB3	44 33 46.29685	121 32 56.15898	1179.887
SIS2_IB1	44 24 49.84091	121 45 07.82346	1081.530
SIsters2	44 17 6.32589	121 33 21.56444	957.216

***Table 2.2 continued**. Base Station Surveyed Coordinates for **2010**.*

	Datum NAD83 (HARN)		GRS80
Base Stations ID	**Latitude (North)**	**Longitude (West)**	**Ellipsoid Height (m)**
3FJ_01	44 26 44.81912	121 46 46.17402	1292.511
AD9193	43 52 10.29925	121 27 22.07928	1247.736
AR_PWH1	43 39 50.63378	121 30 27.01222	1267.949
AR_PWH2	43 42 30.82766	121 31 33.70042	1272.459
China Hat 1	43 51 16.53733	121 06 12.45141	1409.420
China Hat 2	43 47 57.53358	121 00 21.46747	1401.952
China Hat 4	43 39 36.37642	120 50 50.34971	1530.983
China Hat 5	43 29 23.42275	121 03 15.98832	1354.250
CL_DB1	43 58 48.63113	121 31 14.42360	1602.116
CL3_AW1	43 52 18.84340	121 27 26.18486	1246.968
CL3_DB2	43 58 45.87969	121 30 46.67609	1592.403
CL3_DB4	43 56 49.54149	121 36 05.95067	1595.515
CL3_DB5	43 53 26.35760	121 34 23.85087	1328.108
CL3_DB6	43 53 26.22688	121 34 23.36053	1328.016
CL3_DB7	44 01 17.70630	121 22 01.03065	1160.175
CL3_PWH1	43 50 57.47490	121 32 27.64700	1308.667
CL4_DB1	43 45 16.21200	121 34 24.59759	1277.331
CL4_DB2	43 44 21.63368	121 37 51.06188	1291.539
CL6_CB_01	43 16 46.83888	121 49 48.26069	1532.563
CL6_DB1	43 22 16.05575	121 49 43.73159	1427.186
CL6_EG1	43 20 14.66889	121 51 27.23403	1456.314
CL6_LJ1	43 21 36.87373	121 50 53.89536	1458.876
CL6_RG1	43 20 14.66851	121 51 27.23345	1456.325
CL6_RI1	43 31 45.45490	121 56 50.29620	1433.901
CL6_RI2	43 30 37.29478	121 58 11.09399	1435.572
DA_DB1	44 8 7.40991	120 43 36.67908	1053.103
DA_DB2	44 16 06.78328	121 11 58.23563	898.107
DA_DB3	44 16 42.37582	121 12 25.86302	885.921
DA_DB4	44 16 42.38773	121 12 26.37018	885.848
DA_DB5	44 7 14.92788	121 19 3.65407	1023.762
JACK_01	43 12 50.23290	121 37 10.90309	1576.463
JACK_02	43 11 19.54846	121 32 57.93613	1512.609
JACK_03	43 11 12.54826	121 32 50.01047	1513.491
JACK_04	43 19 07.80212	121 30 52.54466	1643.444
JACK_05	43 15 49.33136	121 35 18.61995	1619.393
NGS_S21C	43 52 10.42129	121 27 21.97904	1247.666
PV3_IB4	44 16 36.11242	120 44 53.73911	1072.697
Sisters_01	44 01 41.78953	121 43 54.67823	1635.938
Sisters_02	44 02 34.47069	121 39 53.94907	2046.817
TCSP2	44 8 59.52851	121 27 5.94067	1050.741

For data delivered to date, 24,452 RTK (Real-time kinematic) points were collected in the study area. **Figures 2.3 - 2.13** show detailed views of selected RTK locations for the areas delivered to date.

Figure 2.3. *Selected RTK point locations in the study area for delivery area 1; images are NAIP orthophotos.*

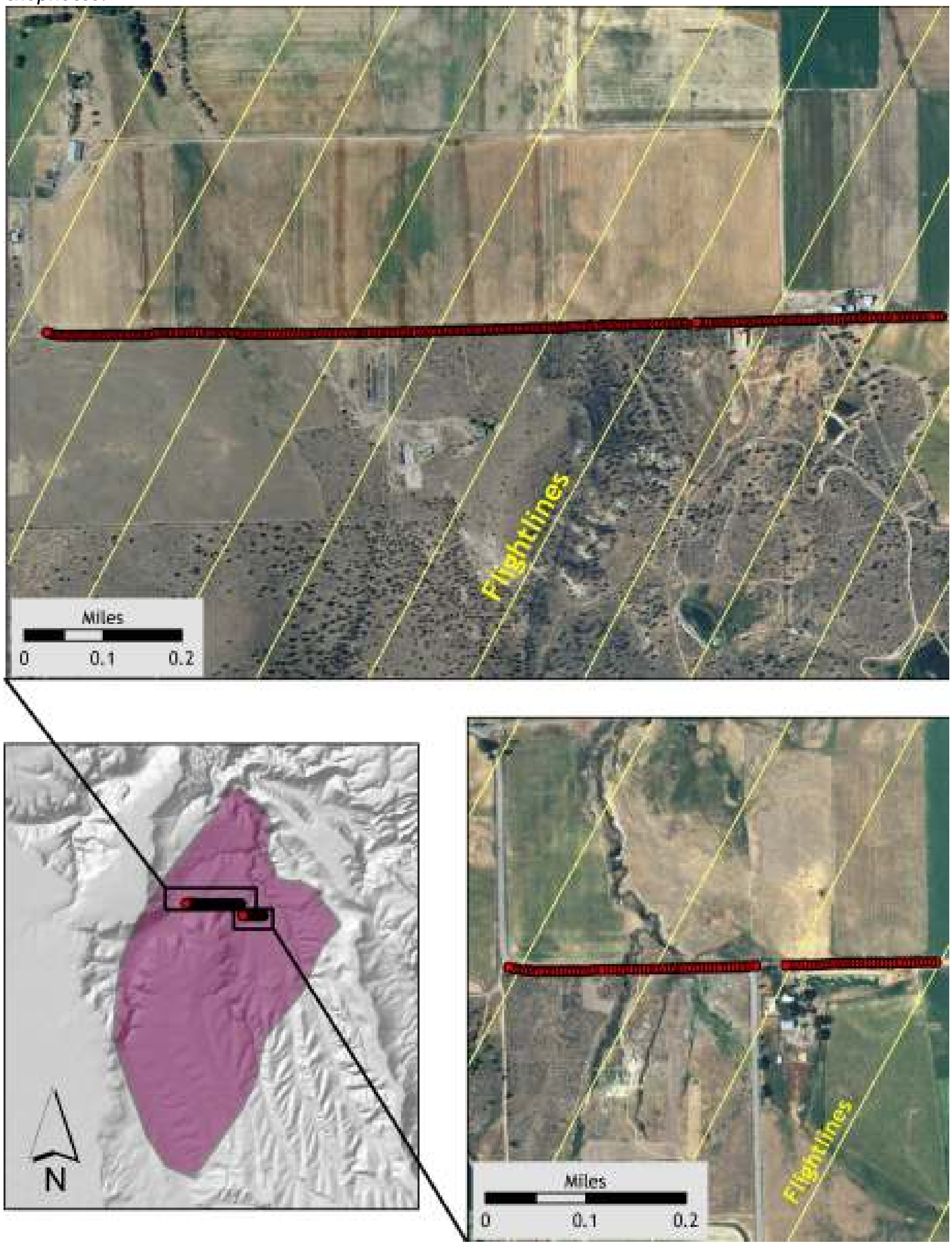

Figure 2.4. *Selected RTK point locations in the study area for delivery area 2; images are NAIP orthophotos.*

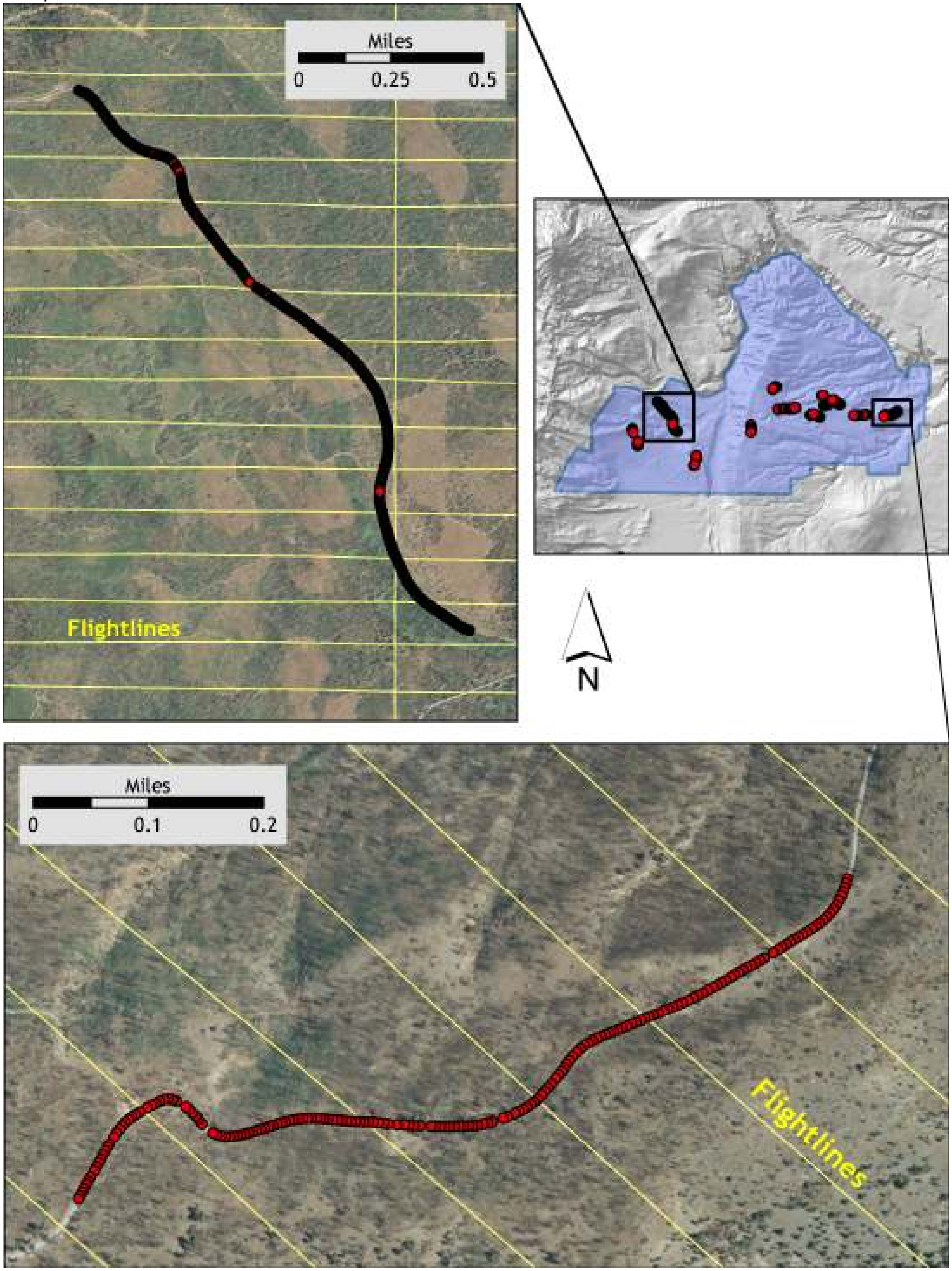

Figure 2.5. *Selected RTK point locations in the study area for deliveries 3 and 5; images are NAIP orthophotos.*

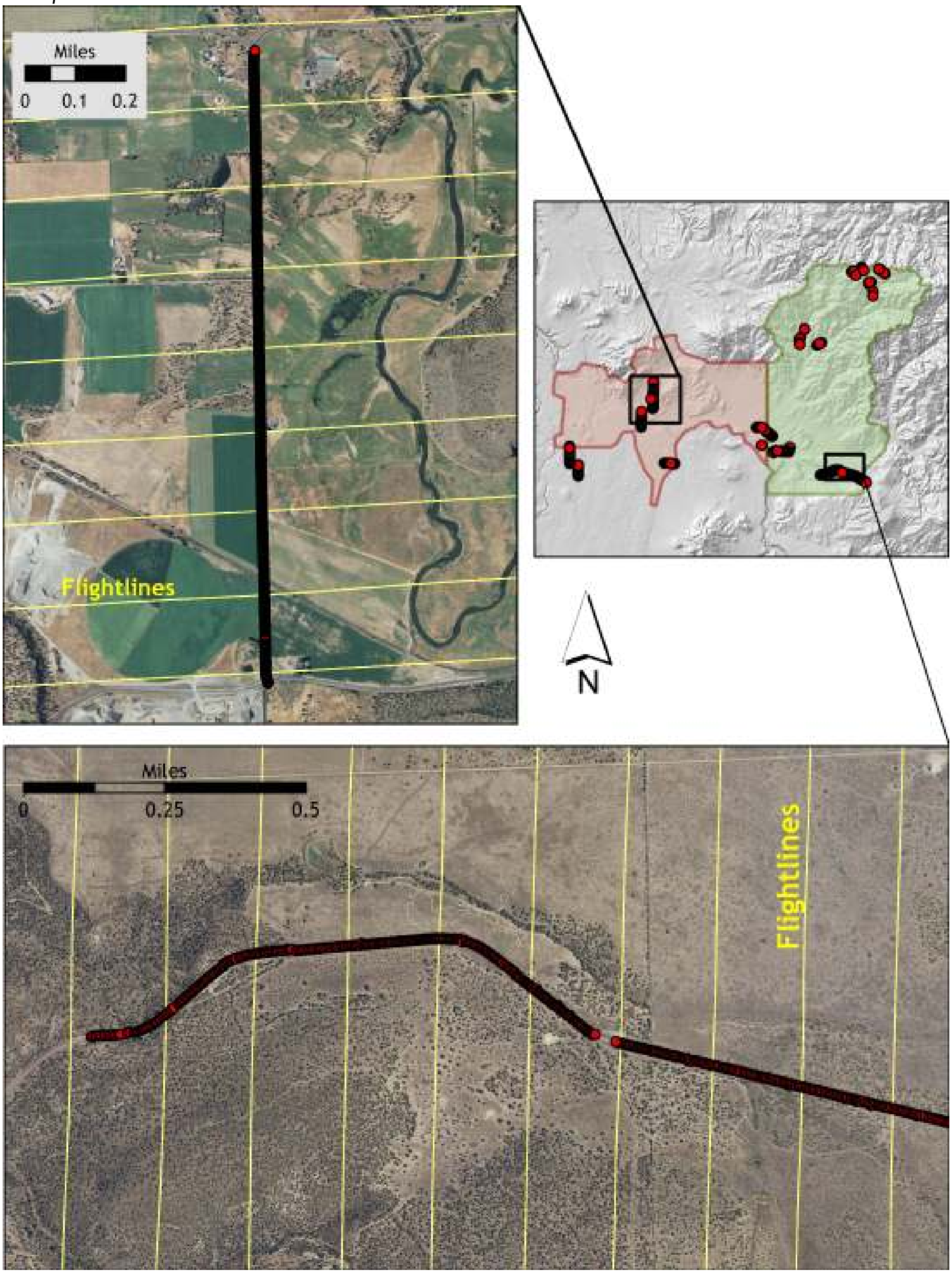

Figure 2.6. *Selected RTK point locations in the study area for delivery area 4; images are NAIP orthophotos.*

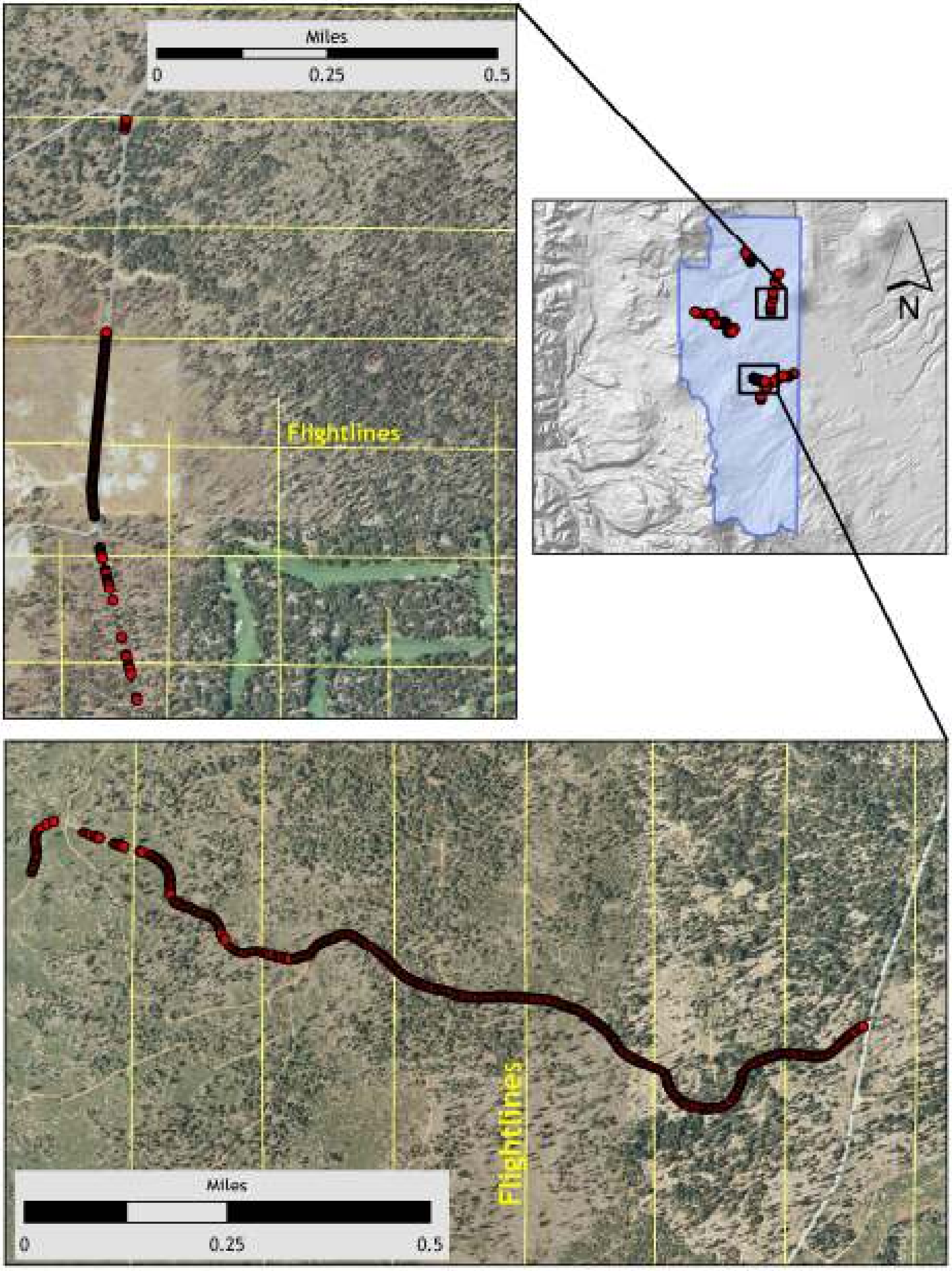

Figure 2.7. *Selected RTK point locations in the study area for delivery area 6; images are NAIP* orthophotos.

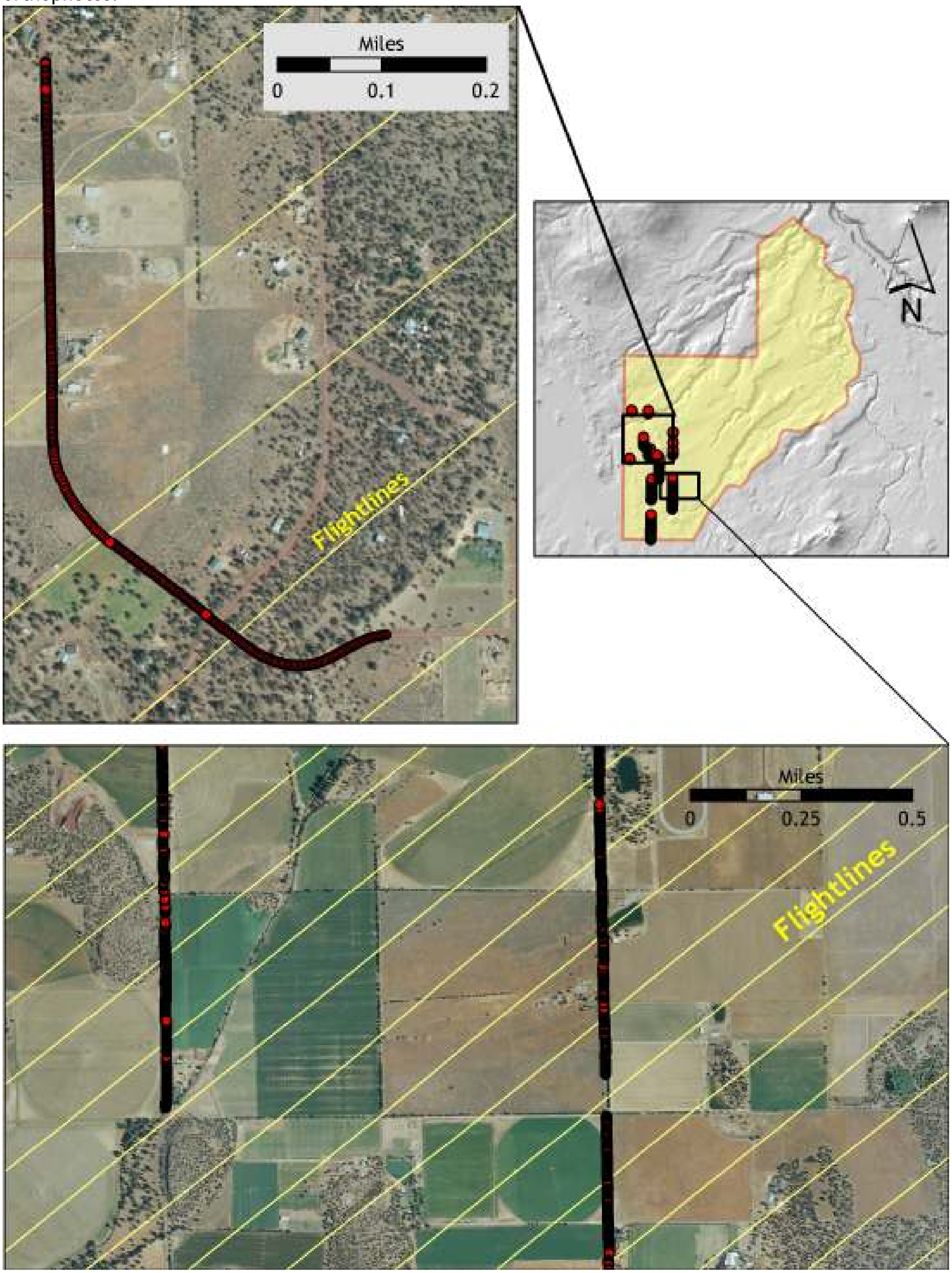

Figure 2.8. *Selected RTK point locations in the study area for delivery area 7; images are NAIP orthophotos.*

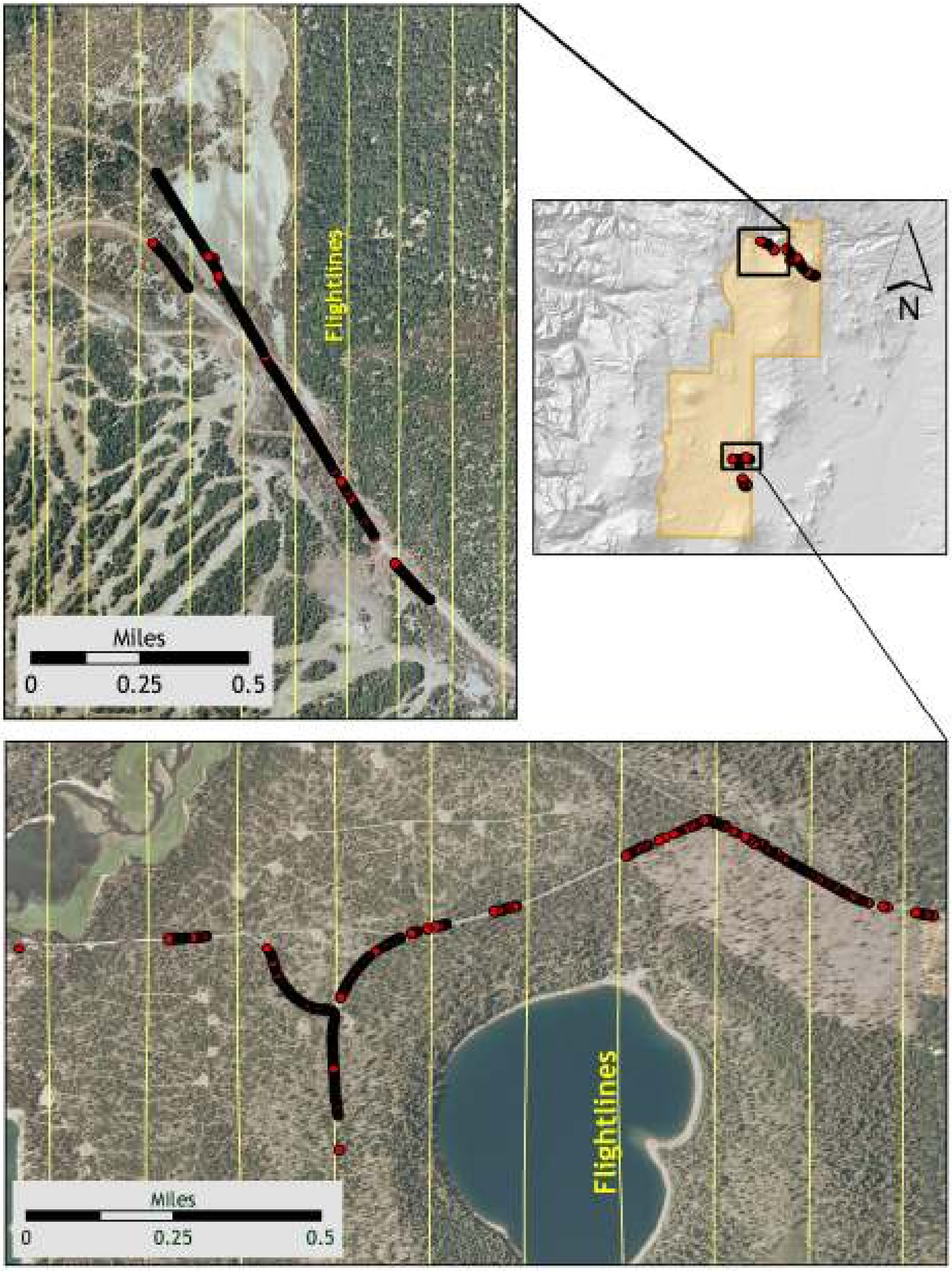

Figure 2.9. *Selected RTK point locations in the study area for delivery area 8; images are NAIP orthophotos.*

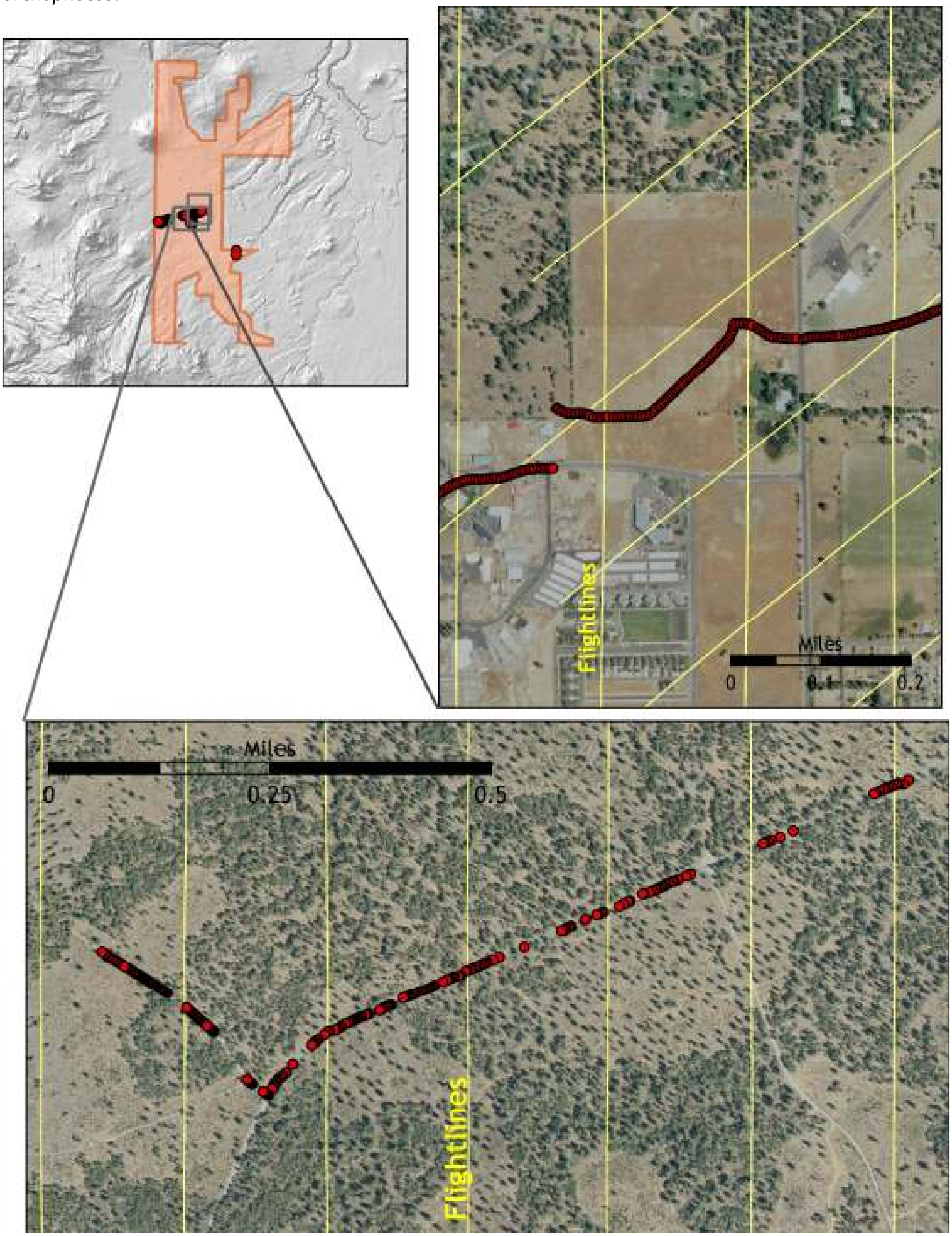

Figure 2.10. *Selected RTK point locations in the study area for delivery area 9; images are NAIP orthophotos.*

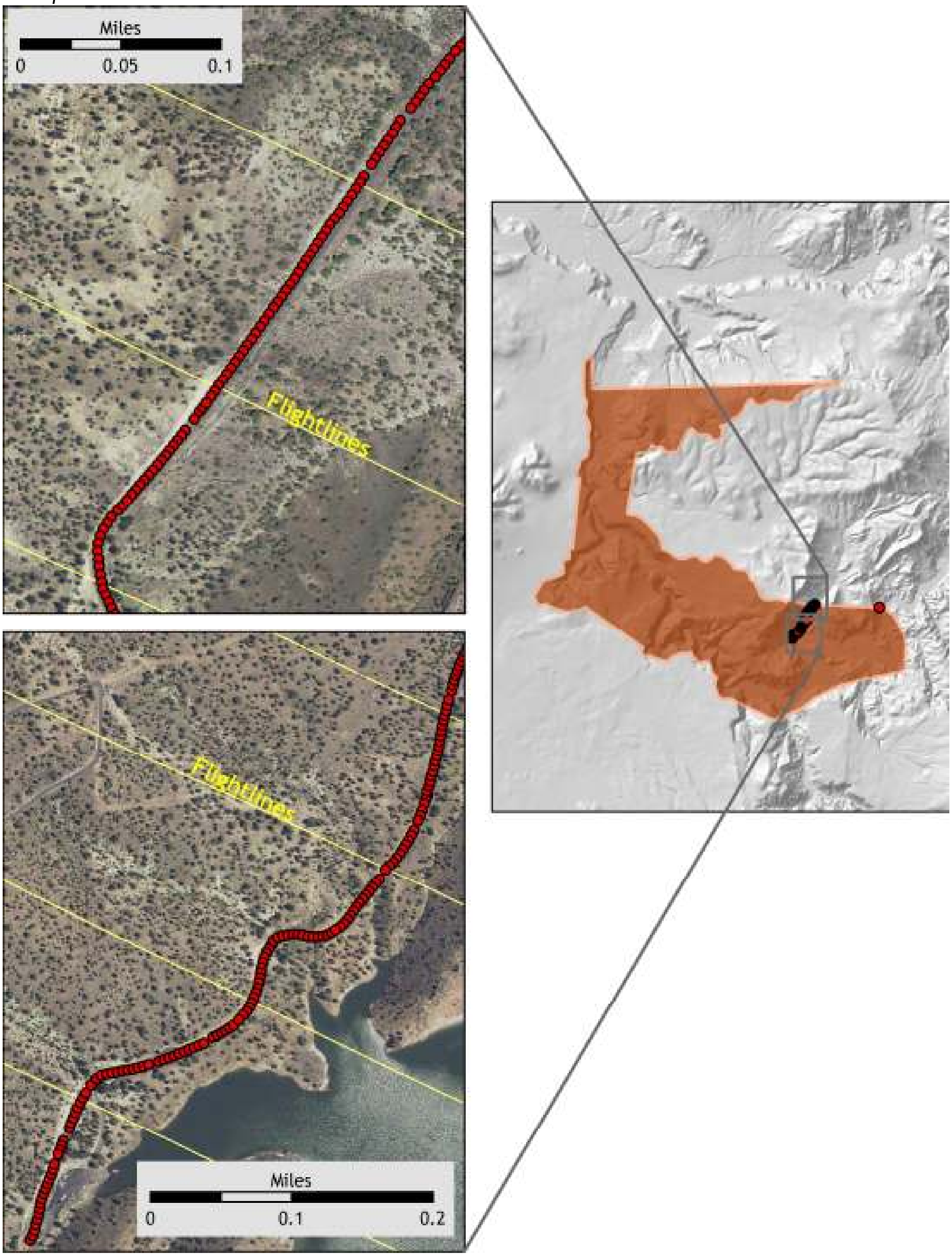

Figure 2.11. *Selected RTK point locations in the study area for delivery area 10; images are NAIP orthophotos.*

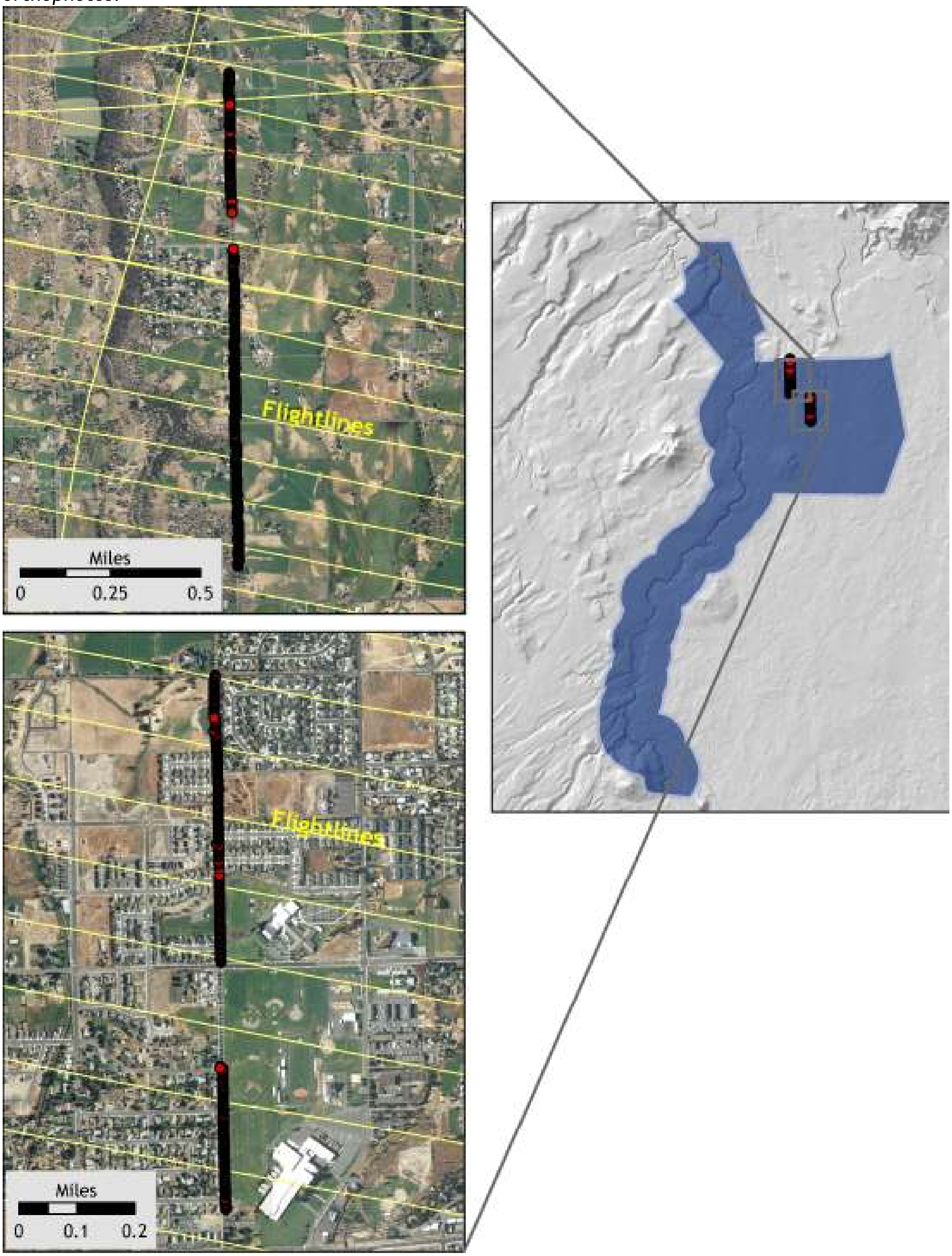

Figure 2.12. *Selected RTK point locations in the study area for delivery area 11; images are NAIP orthophotos.*

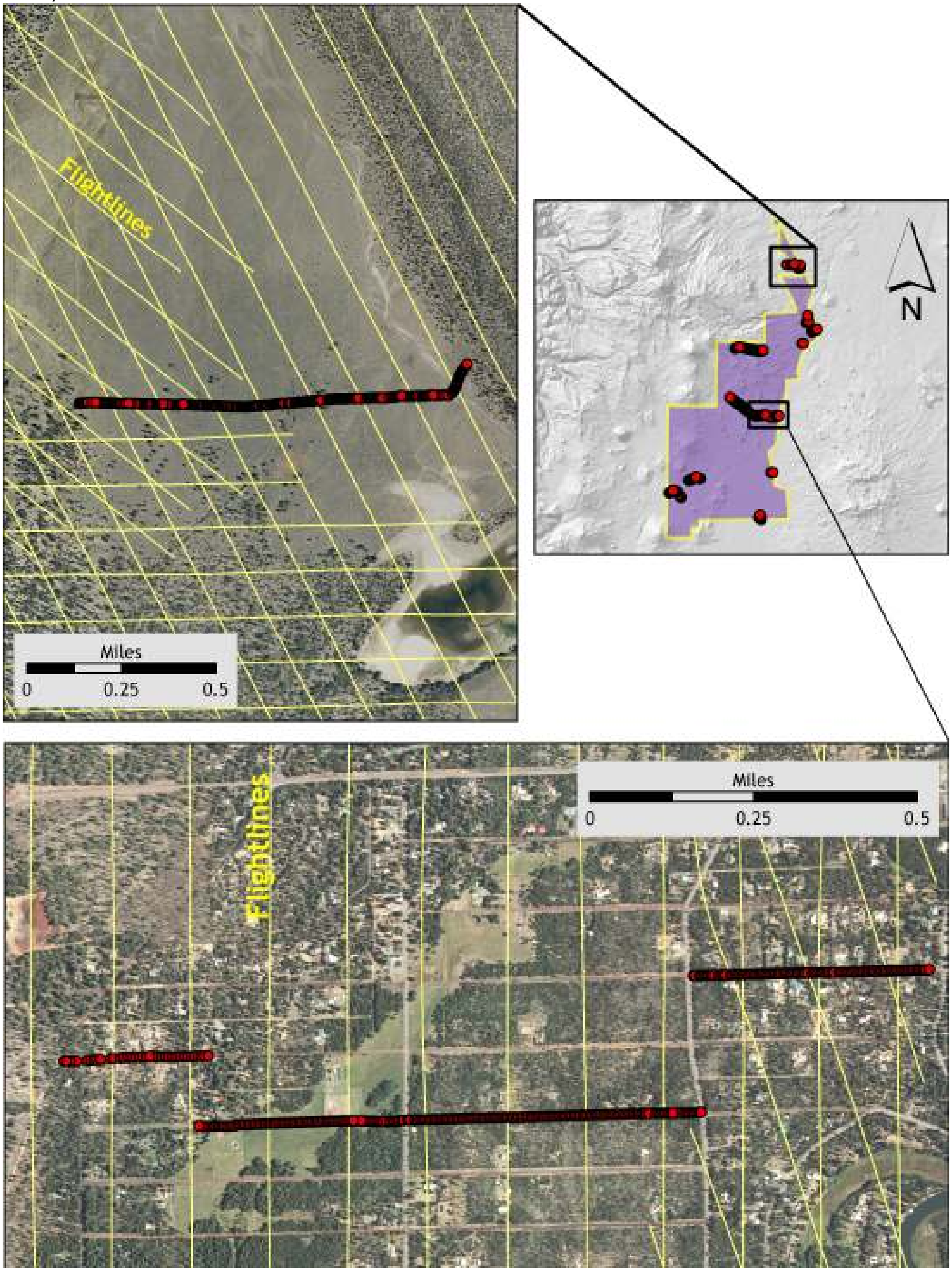

Figure 2.13. *Selected RTK point locations in the study area for delivery area 12; images are NAIP orthophotos.*

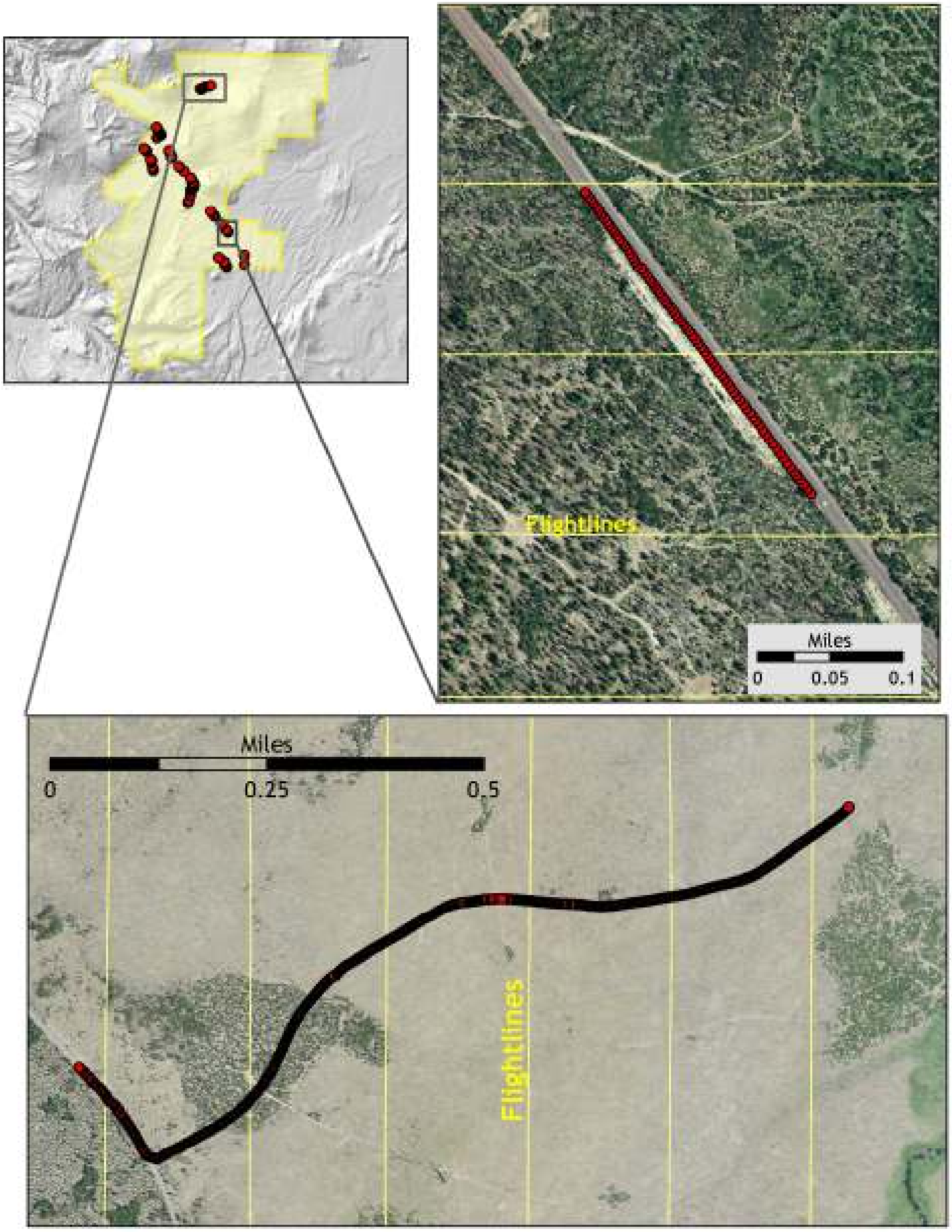

3. Accuracy

3.1 Relative Accuracy

Relative Accuracy Calibration Results

Relative accuracy refers to the internal consistency of the data set and is measured as the divergence between points from different flightlines within an overlapping area. Divergence is most apparent when flightlines are opposing. When the LiDAR system is well calibrated, the line to line divergence is low (<10 cm). Internal consistency is affected by system attitude offsets (pitch, roll and heading), mirror flex (scale), and GPS/IMU drift.

Relative accuracy statistics are based on the comparison of 2,137 flightlines and over 63 billion points. Relative accuracy is reported for the portion of the study area shown in **Figure 3.1** below and the deviation statistics are reported in **Figures 3.2** and **3.3**.

- Project Average = 0.15 ft (0.04 m)
- Median Relative Accuracy = 0.14 ft (0.04 m)
- 1σ Relative Accuracy = 0.15 ft (0.05m)
- 2σ Relative Accuracy = 0.21 ft (0.06 m)

***Figure 3.1**. Relative Accuracy Covered Area.*

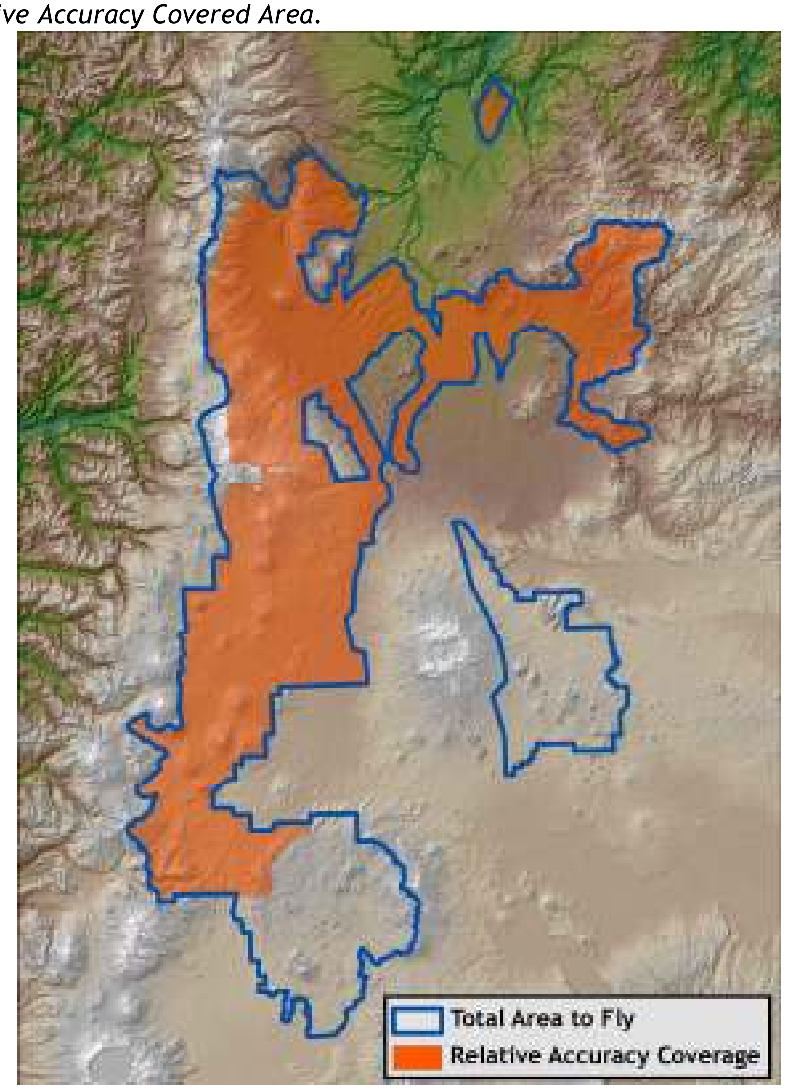

Figure 3.2. Statistical relative accuracies, non slope-adjusted.

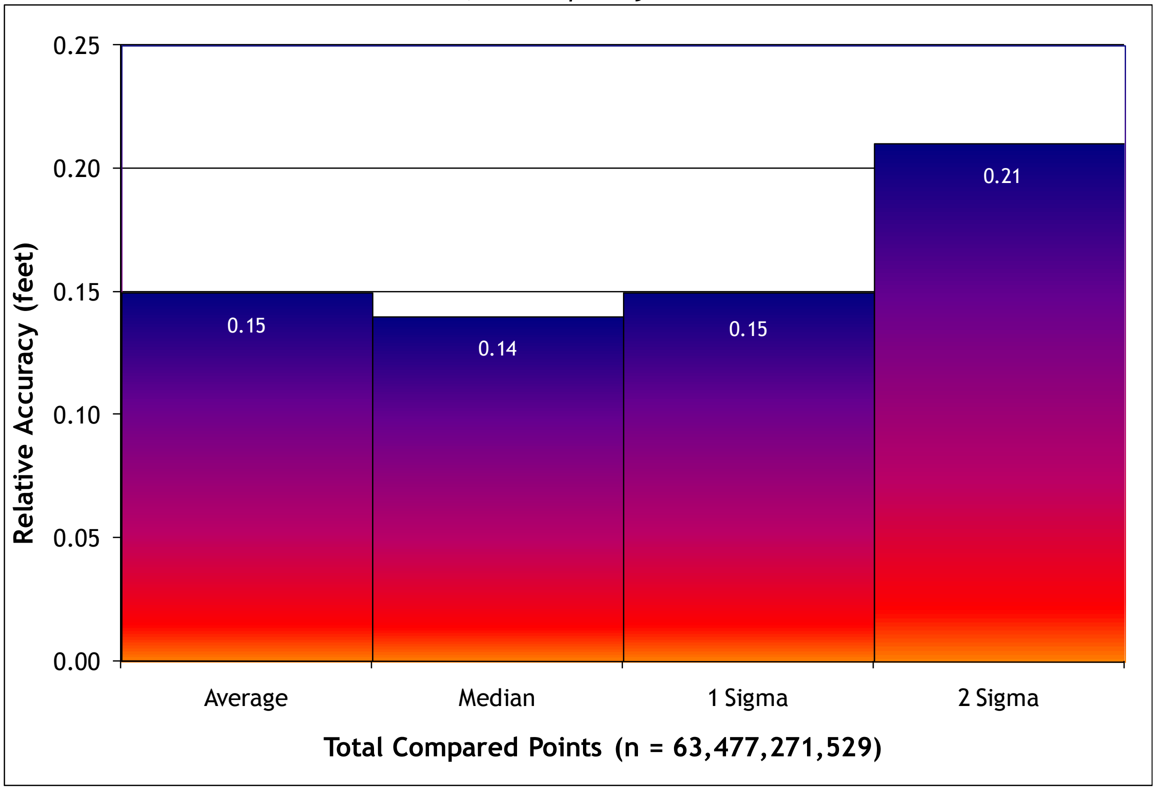

Figure 3.3. Percentage distribution of relative accuracies, non slope-adjusted.

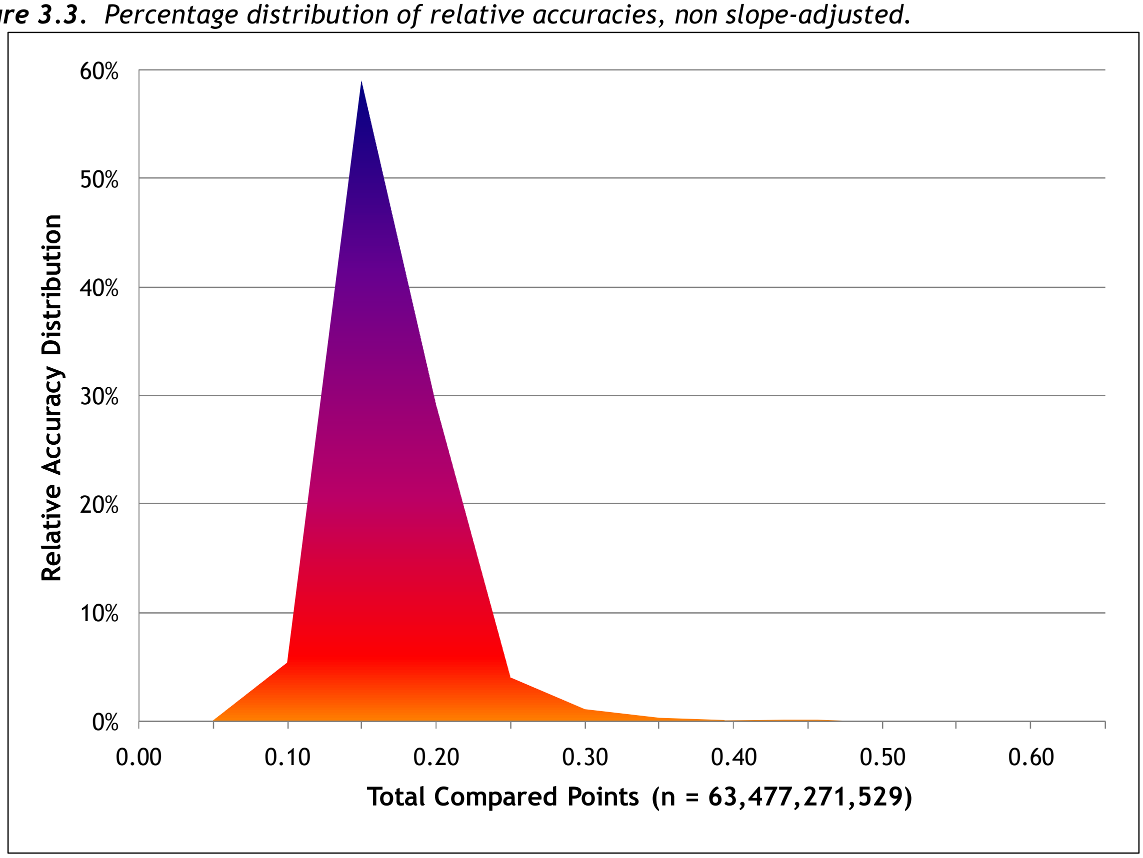

3.2 Absolute Accuracy

Absolute accuracy compares known RTK ground survey points to the closest laser point. For the Deschutes Study Area, 24,452 RTK points were collected for data delivered to date. Absolute accuracy is reported for the portion of the study area shown in **Figure 3.4** and reported in **Table 3.1** below. Histogram and absolute deviation statistics are reported in **Figures 3.5 and 3.6**.

Table 3.1. *Absolute Accuracy – Deviation between laser points and RTK survey points.*

Sample Size (n): 24,452	
Root Mean Square Error (RMSE): 0.12 ft (0.04m)	
Standard Deviations	**Deviations**
1 sigma (σ): 0.11 ft (0.03 m)	**Minimum Δz:** -0.58 ft (-0.18 m)
2 sigma (σ): 0.25 ft (0.08 m)	**Maximum Δz:** 0.51 ft (0.16 m)
	Average Δz: 0.09 ft (0.03 m)

Figure 3.4. *Absolute Accuracy Covered Area.*

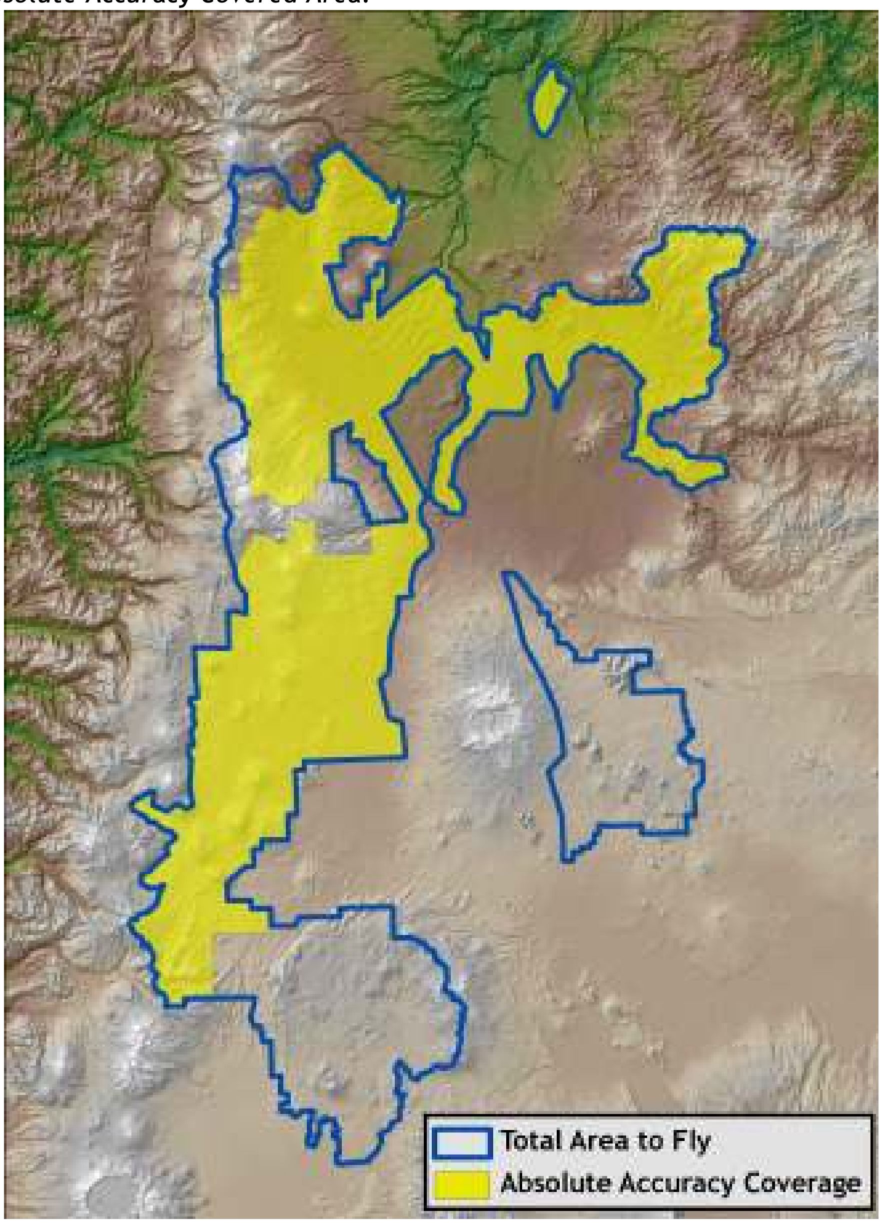

Figure 3.5. Deschutes Study Area histogram statistics

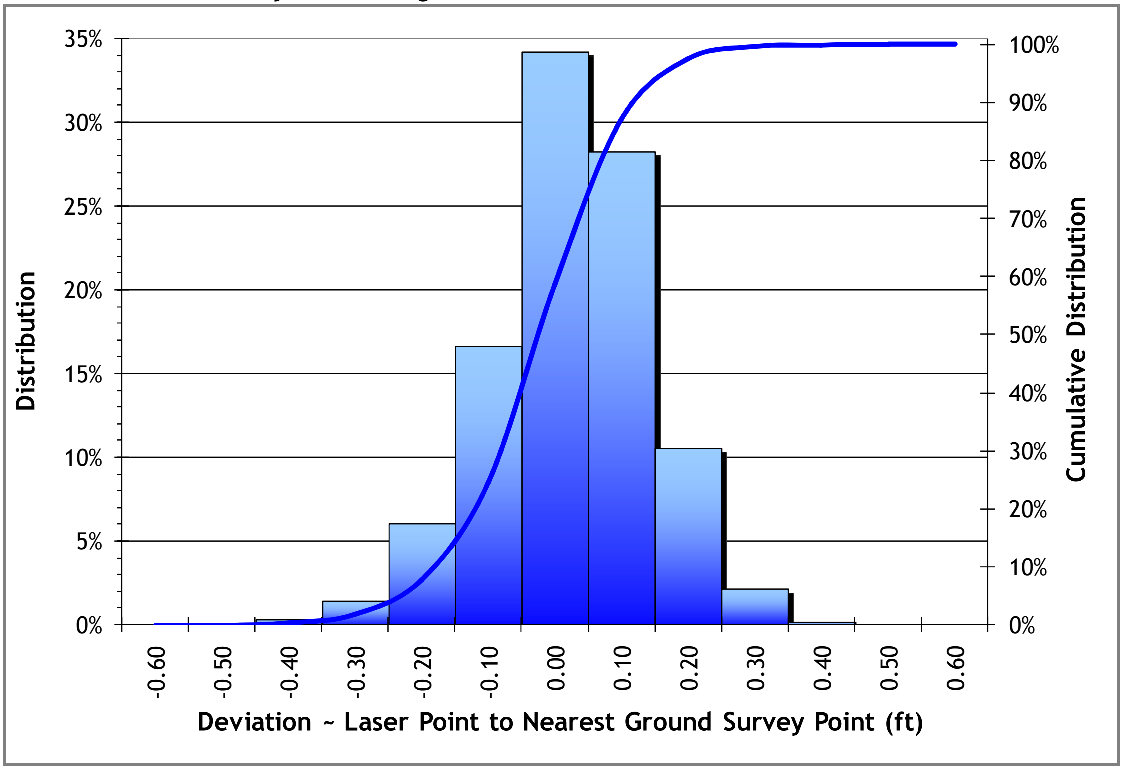

Figure 3.6. Deschutes Study Area point absolute deviation statistics.

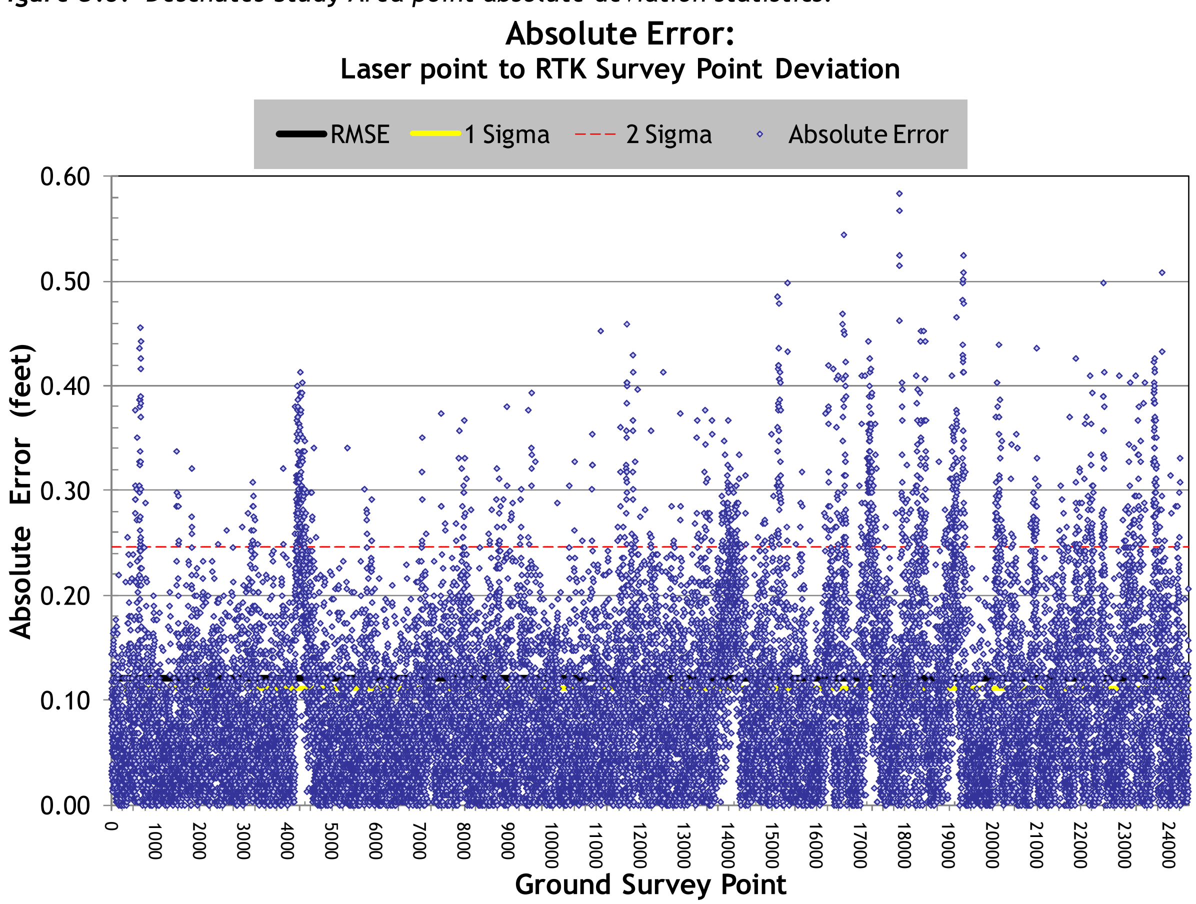

4. Data Density/Resolution

4.1 Density Statistics

Some types of surfaces (i.e. dense vegetation or water) may return fewer pulses than the laser originally emitted. Therefore, the delivered density can be less than the native density and vary according to terrain, land cover and water bodies. Density histograms and maps (**Figures 4.1 – 4.4**) have been calculated based on first return laser point density and ground-classified laser point density.

Table 4.1. *Average density statistics for Deschutes Study Area data delivered to date.*

Average Pulse Density (per square ft)	Average Pulse Density (per square m)	Average Ground Density (per square ft)	Average Ground Density (per square m)
0.86	9.3	.22	2.4

Figure 4.1. *Histogram of first return laser point density for data delivered to date.*

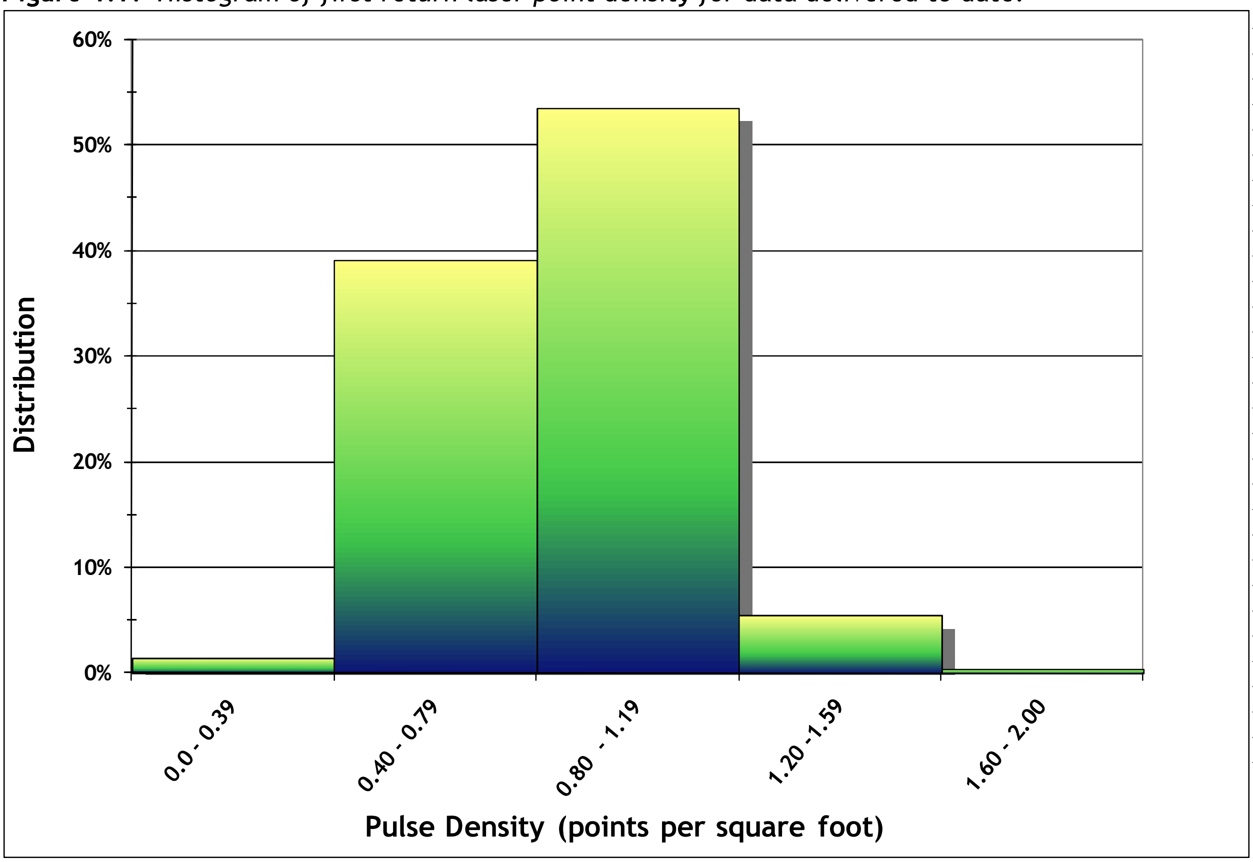

Pts ft²	Pts m²
0.00	0.00
0.05	0.54
0.10	1.08
0.15	1.61
0.20	2.15
0.25	2.69
0.30	3.23
0.35	3.77
0.40	4.31
0.45	4.84
0.50	5.38
0.55	5.92
0.60	6.46
0.65	7.00
0.70	7.53
0.75	8.07
0.80	8.61
0.85	9.15
0.90	9.69
0.95	10.23
1.00	10.76
1.05	11.30
1.10	11.84
1.15	12.38
1.20	12.92
1.25	13.45
1.30	13.99
1.35	14.53
1.40	15.07
1.45	15.61
1.50	16.15

Figure 4.2. F*irst return laser point densities per 0.75' USGS Quad for data delivered to date.*

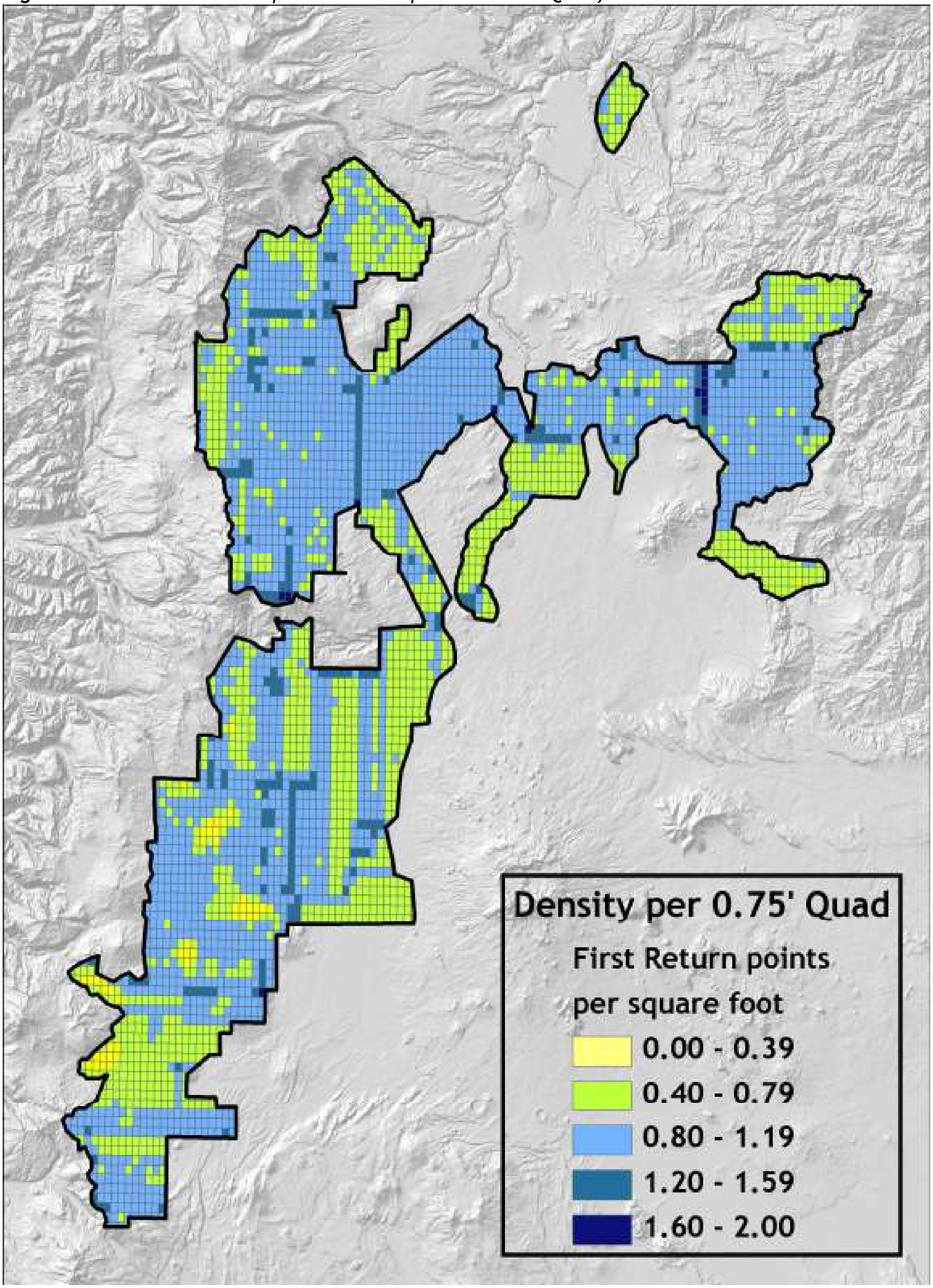

Pts ft^2	Pts m^2
0.00	0.00
0.05	0.54
0.10	1.08
0.15	1.61
0.20	2.15
0.25	2.69
0.30	3.23
0.35	3.77
0.40	4.31
0.45	4.84
0.50	5.38
0.55	5.92
0.60	6.46
0.65	7.00
0.70	7.53
0.75	8.07
0.80	8.61
0.85	9.15
0.90	9.69
0.95	10.23
1.00	10.76
1.05	11.30
1.10	11.84
1.15	12.38
1.20	12.92
1.25	13.45
1.30	13.99
1.35	14.53
1.40	15.07
1.45	15.61
1.50	16.15

Ground classifications were derived from ground surface modeling. Classifications were performed by reseeding of the ground model where it was determined that the ground model failed, usually under dense vegetation and/or at breaks in terrain, steep slopes and at bin boundaries.

Figure 4.3. *Histogram of ground-classified laser point density for data delivered to date.*

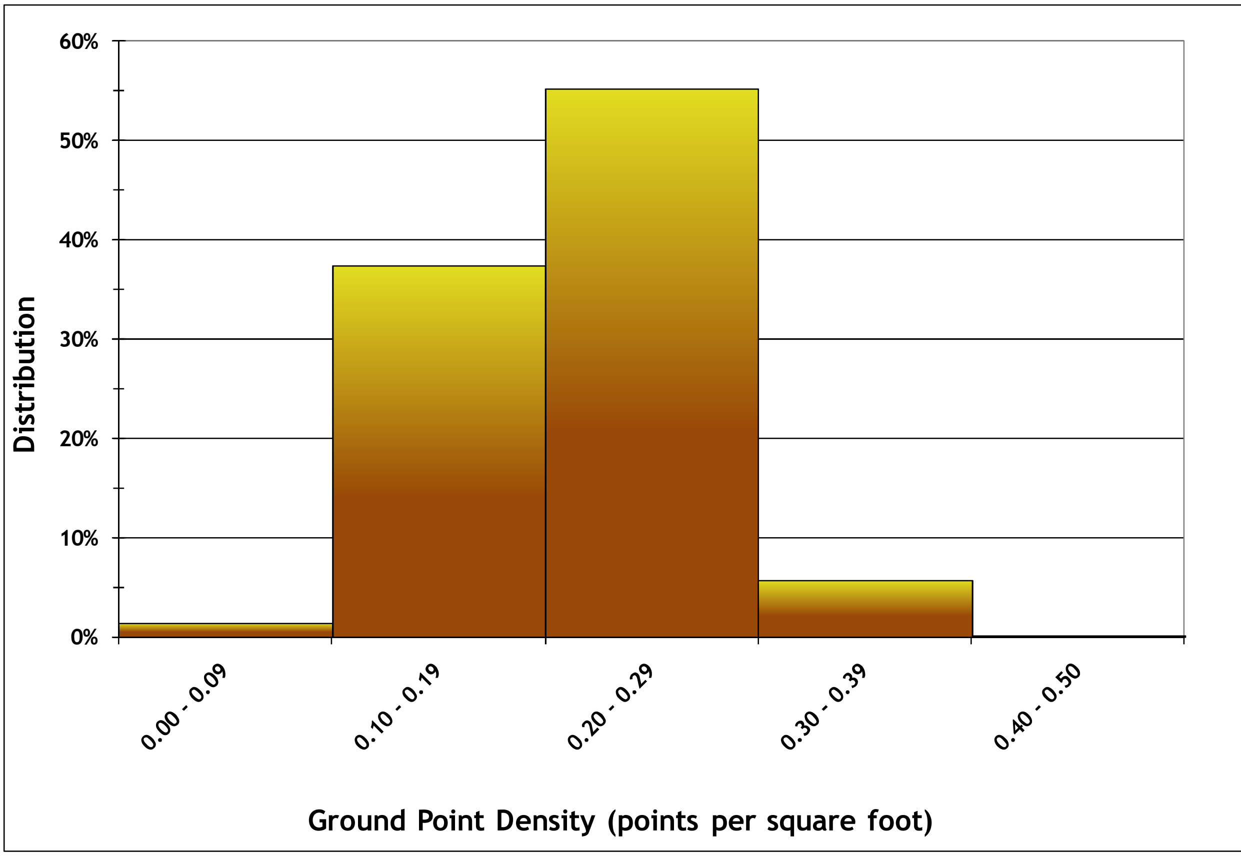

Pts ft^2	Pts m^2
0.00	0.00
0.05	0.54
0.10	1.08
0.15	1.61
0.20	2.15
0.25	2.69
0.30	3.23
0.35	3.77
0.40	4.31
0.45	4.84
0.50	5.38
0.55	5.92
0.60	6.46
0.65	7.00
0.70	7.53
0.75	8.07
0.80	8.61
0.85	9.15
0.90	9.69
0.95	10.23
1.00	10.76
1.05	11.30
1.10	11.84
1.15	12.38
1.20	12.92
1.25	13.45
1.30	13.99
1.35	14.53
1.40	15.07
1.45	15.61
1.50	16.15

Figure 4.4. *Ground-classified laser point density per 0.75' USGS Quad for data delivered to date.*

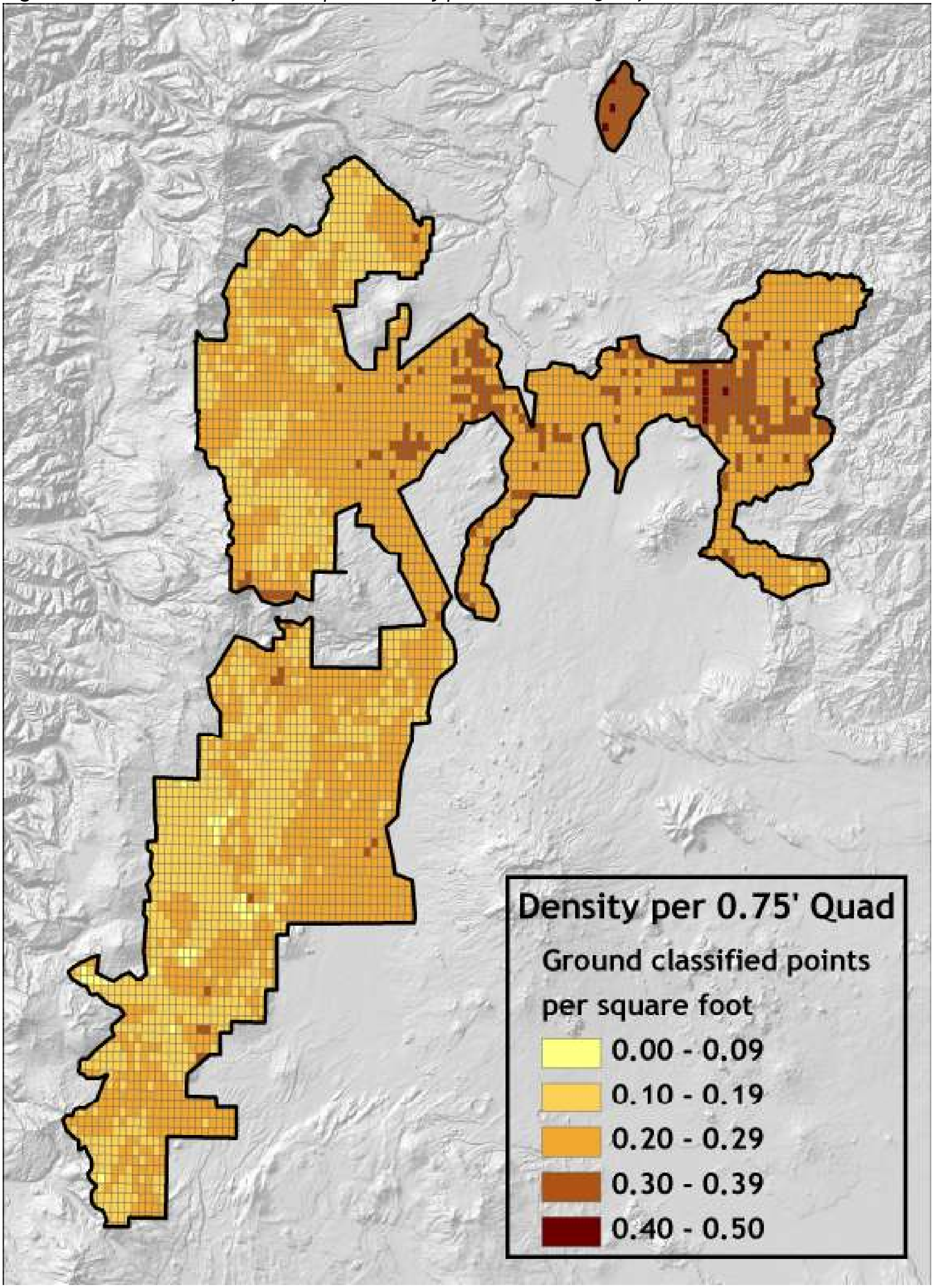

Pts ft²	Pts m²
0.00	0.00
0.05	0.54
0.10	1.08
0.15	1.61
0.20	2.15
0.25	2.69
0.30	3.23
0.35	3.77
0.40	4.31
0.45	4.84
0.50	5.38
0.55	5.92
0.60	6.46
0.65	7.00
0.70	7.53
0.75	8.07
0.80	8.61
0.85	9.15
0.90	9.69
0.95	10.23
1.00	10.76
1.05	11.30
1.10	11.84
1.15	12.38
1.20	12.92
1.25	13.45
1.30	13.99
1.35	14.53
1.40	15.07
1.45	15.61
1.50	16.15

The land cover in the delivery area 1 is almost exclusively agricultural (**Figure 4.5**). This resulted in a high percentage of laser pulses reaching the ground and an exceptionally high ground-point density (an average of 0.34 p/ft^2 (3.67 p/m^2) per 0.75' quad).

Figure 4.5. *Ground-classified point density in delivery area 1 of the Deschutes study area overlaid onto a NAIP orthophoto.*

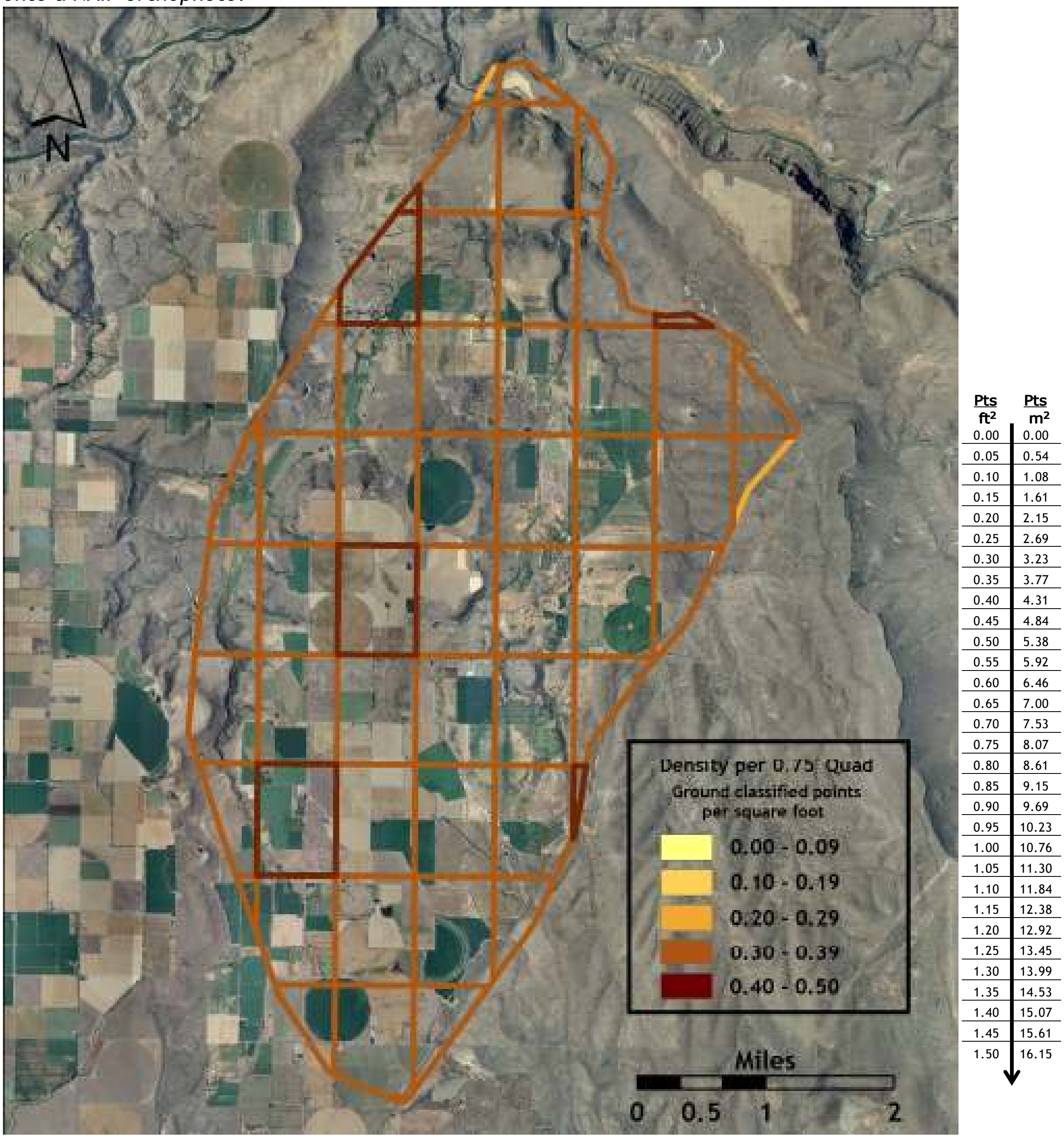

Decreased first-return point density in delivery areas 7 and 11 is due to the low percentage of points returned over water. The main bodies of water causing low pulse density are Crane Prairie Reservoir and Wickiup Reservoir (**Figure 4.6**).

Figure 4.6. *First-return classified point density in delivery areas 7 and 11 of the Deschutes study area overlaid onto a NAIP orthophoto.*

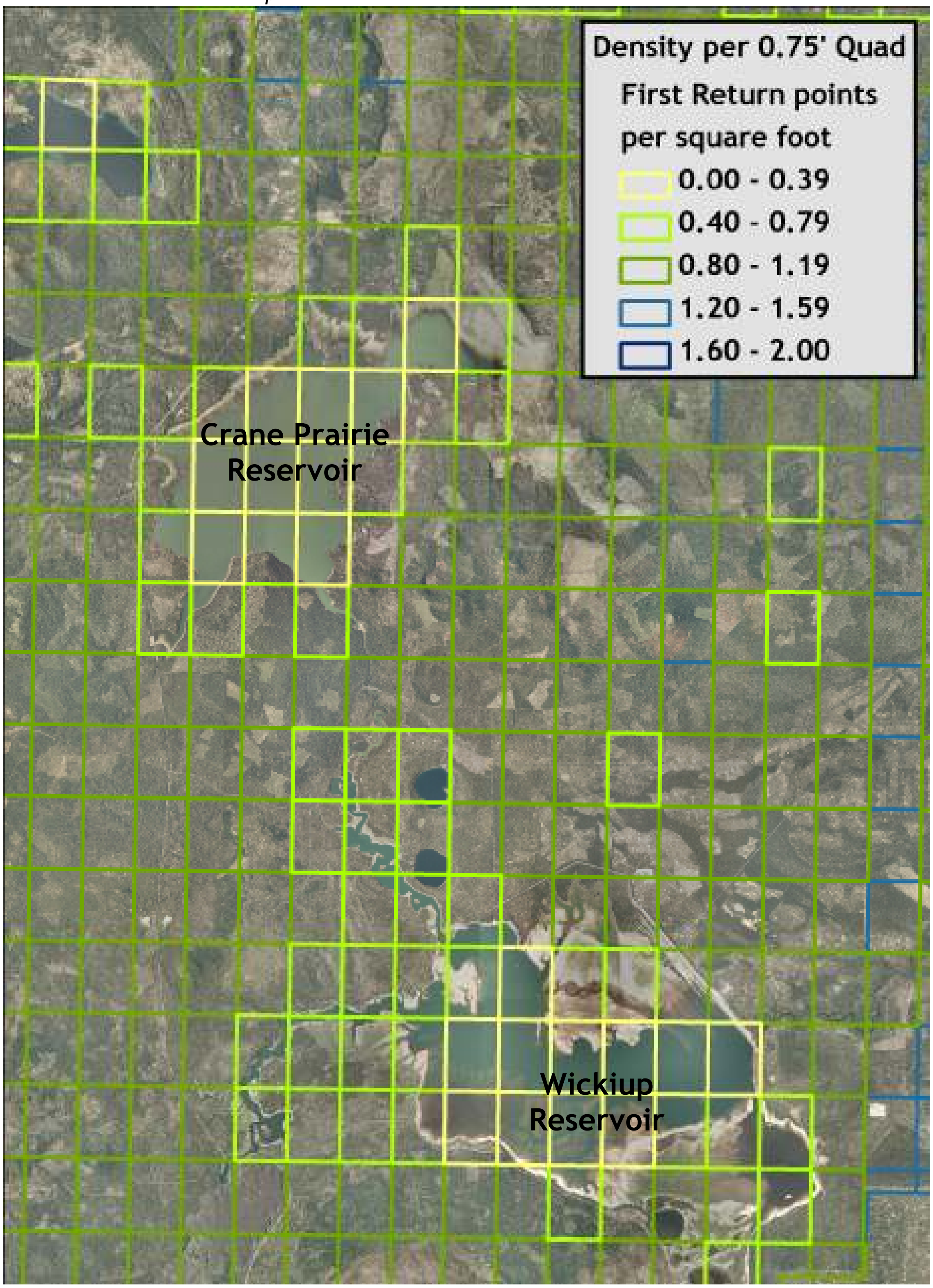

Pts ft²	Pts m²
0.00	0.00
0.05	0.54
0.10	1.08
0.15	1.61
0.20	2.15
0.25	2.69
0.30	3.23
0.35	3.77
0.40	4.31
0.45	4.84
0.50	5.38
0.55	5.92
0.60	6.46
0.65	7.00
0.70	7.53
0.75	8.07
0.80	8.61
0.85	9.15
0.90	9.69
0.95	10.23
1.00	10.76
1.05	11.30
1.10	11.84
1.15	12.38
1.20	12.92
1.25	13.45
1.30	13.99
1.35	14.53
1.40	15.07
1.45	15.61
1.50	16.15

5. Selected Imagery

Figure 5.1. *3-d oblique view of canyon lands north of Old Maid's Canyon and northeast of Madras, OR. The upper image is derived from ground-classified and highest hit LiDAR points while the lower image was created from ground-classified LiDAR points.*

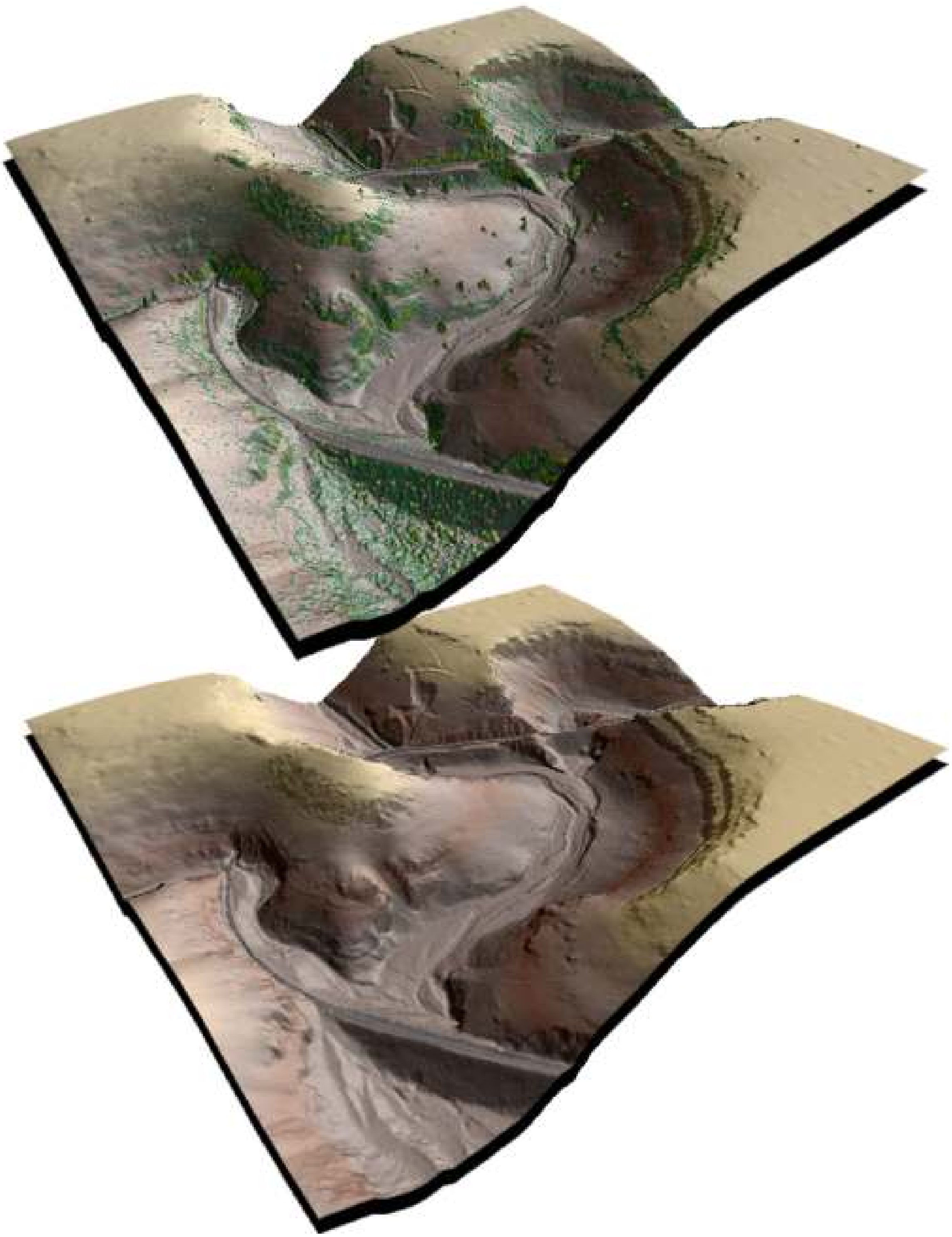

Figure 5.2. *View of Gothic Rock and surrounding area in north central Oregon. Top image derived from highest hit LiDAR, lower image derived from bare earth LiDAR.*

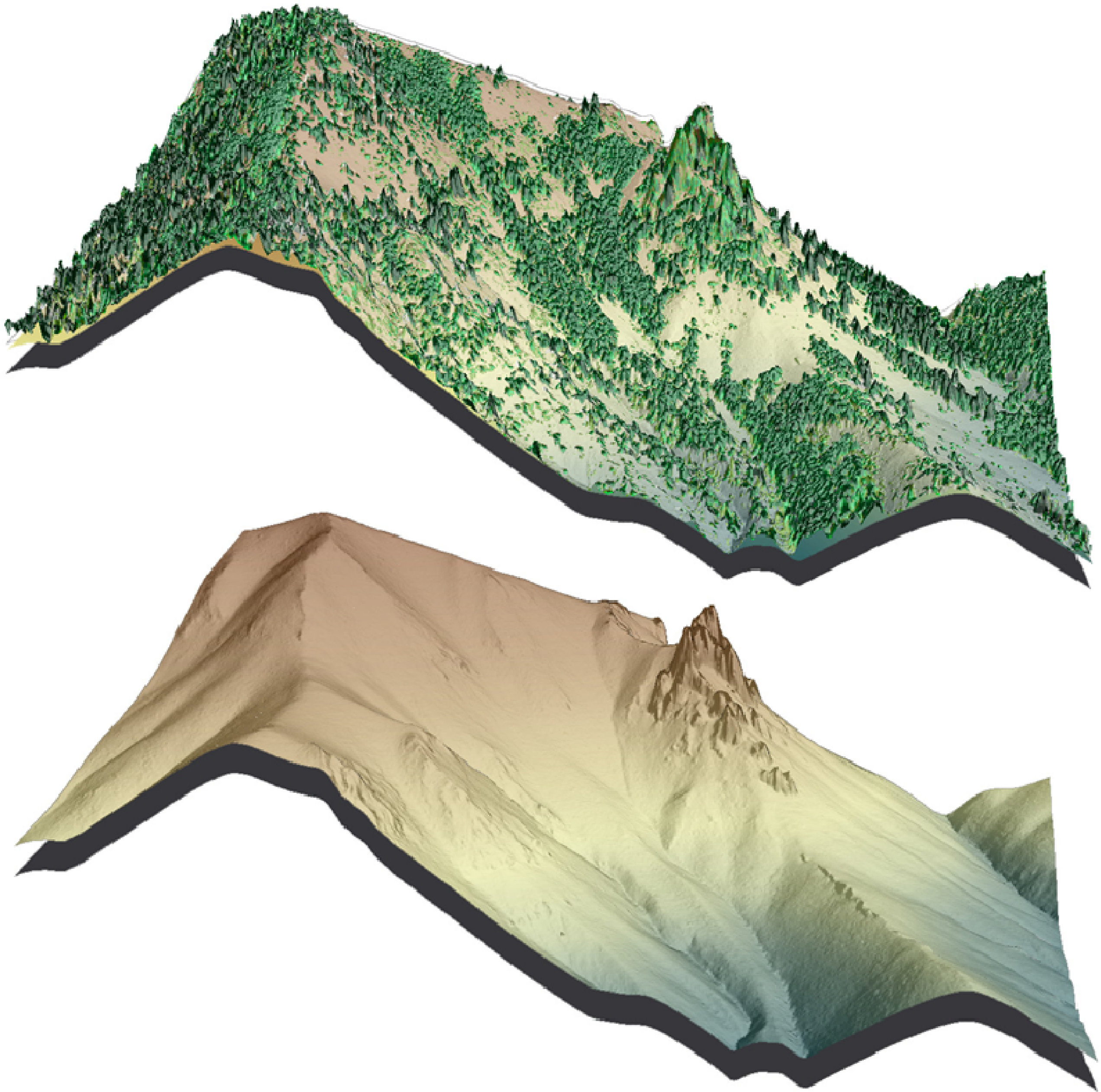

Figure 5.3. *View of forested land north of Hwy 20, along the Metolius River in north central Oregon. Top image derived from highest hit LiDAR, lower image derived from bare earth LiDAR.*

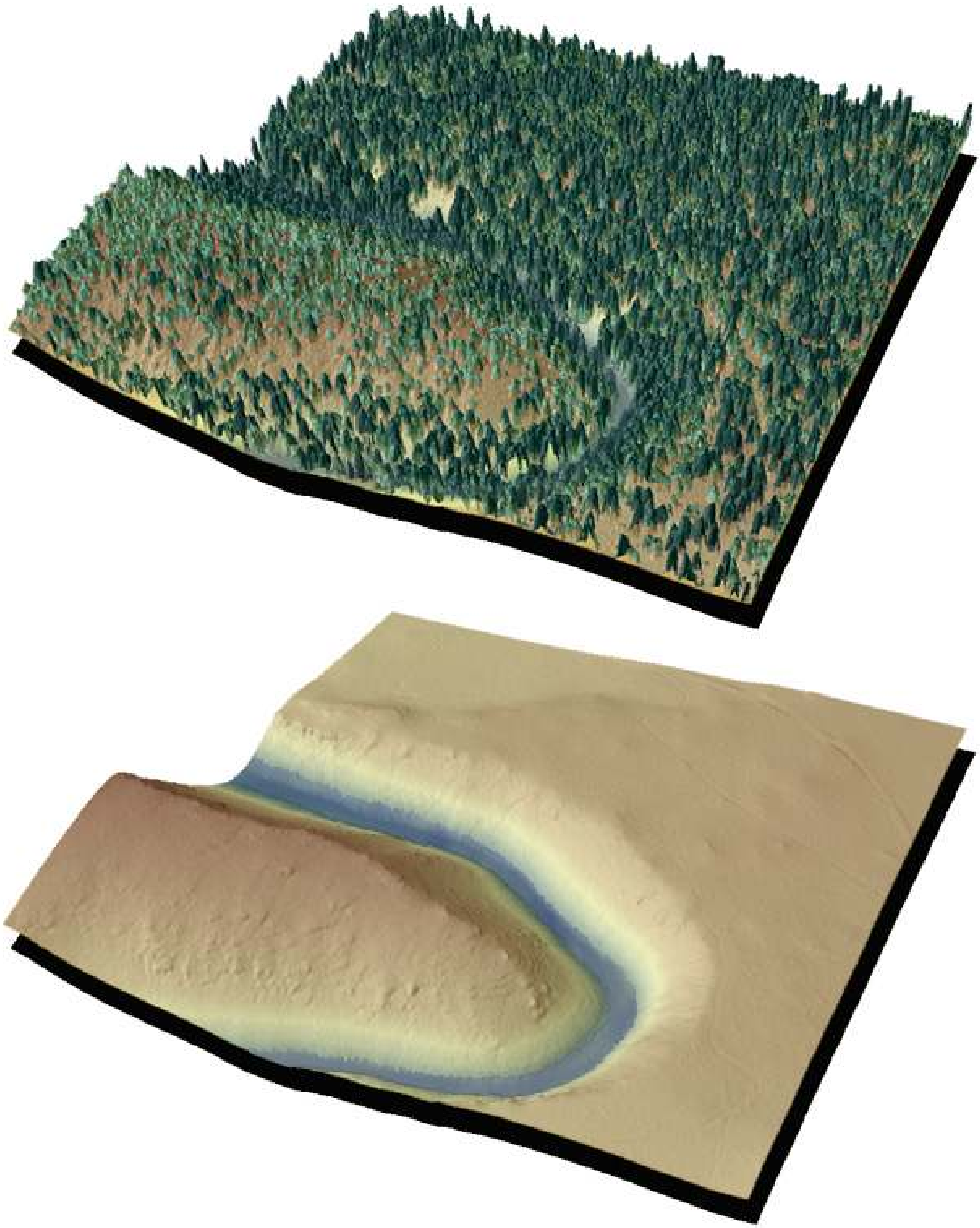

Figure 5.4. *View of Smith Rock State Park and Crooked River, near Terrebonne, OR. Top image is derived from LiDAR highest hits, lower image from NAIP orthophoto draped over highest hit LiDAR.*

Figure 5.5*. The Crooked River near Terrebonne, OR. Top image is derived from highest hit LiDAR, bottom image from bare earth LiDAR.*

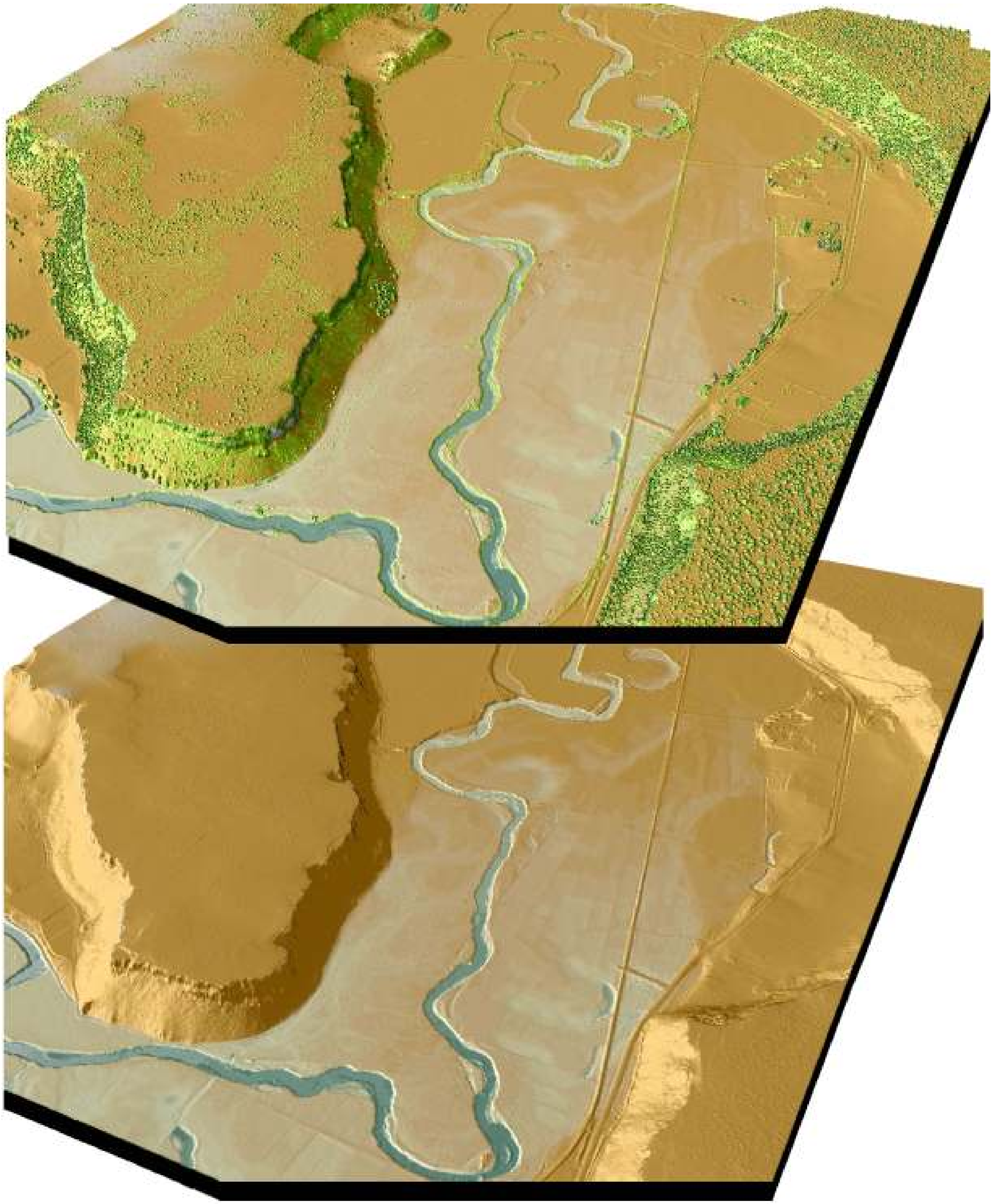

Figure 5.6. *Whychus Creek, near Sisters, Oregon. Image derived from highest hit LiDAR.*

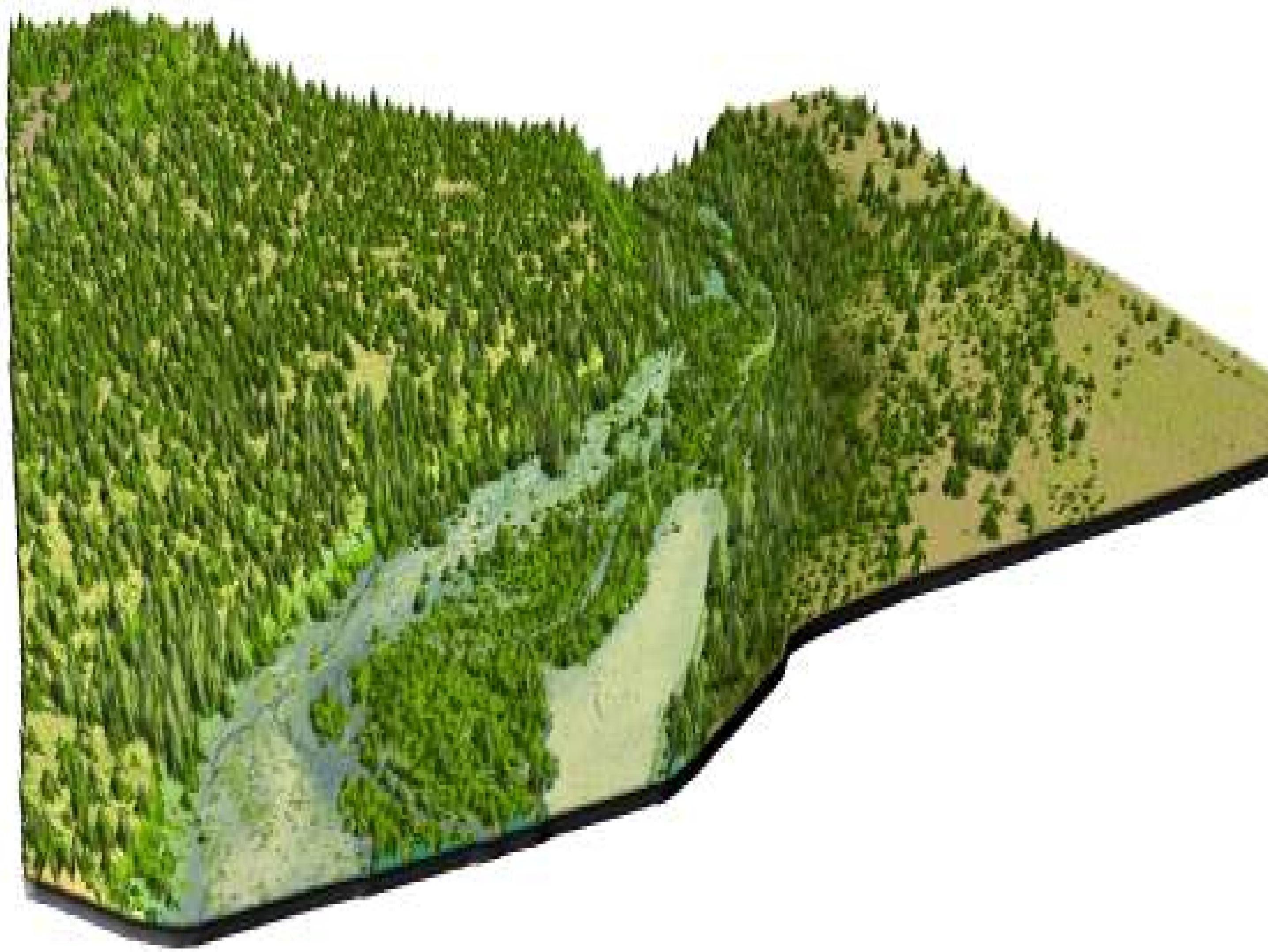

Figure 5.7. Ranch near Sisters, Oregon. Top image derived from highest hit LiDAR, bottom image created from NAIP orthophoto draped over highest hit LiDAR.

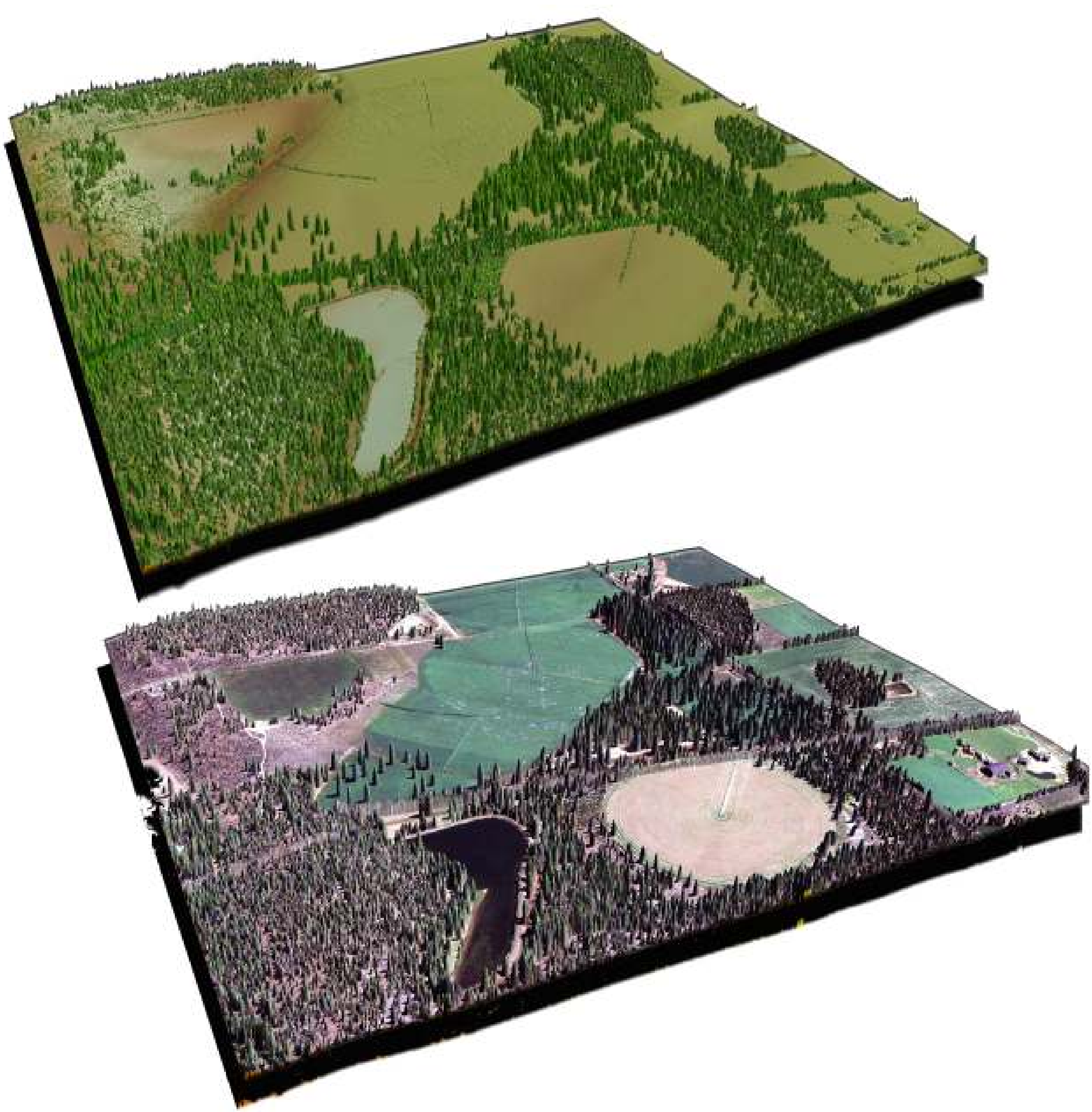

Figure 5.8. *Forested land along State Highway 372, west of the city of Bend. Image created from LiDAR point cloud with RBG values extracted from NAIP orthophoto.*

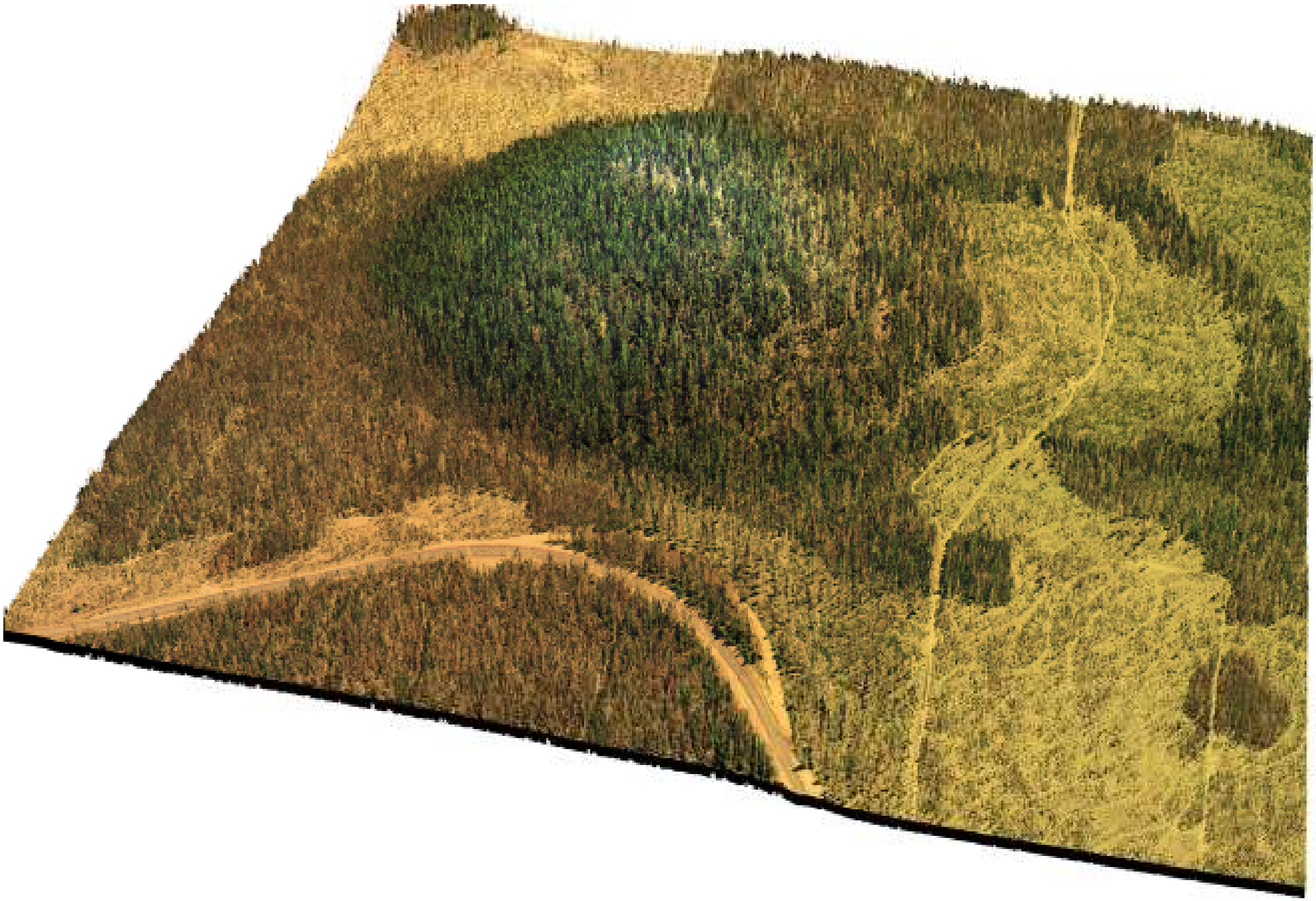

Figure 5.9. *Mount Bachelor, west of the city of Bend. Image created from LiDAR point cloud with RBG values extracted from NAIP orthophoto.*

***Figure 5.10**. Belknap Crater, viewed from the southwest. Image created from LiDAR point cloud with RGB values extracted from NAIP orthophoto.*

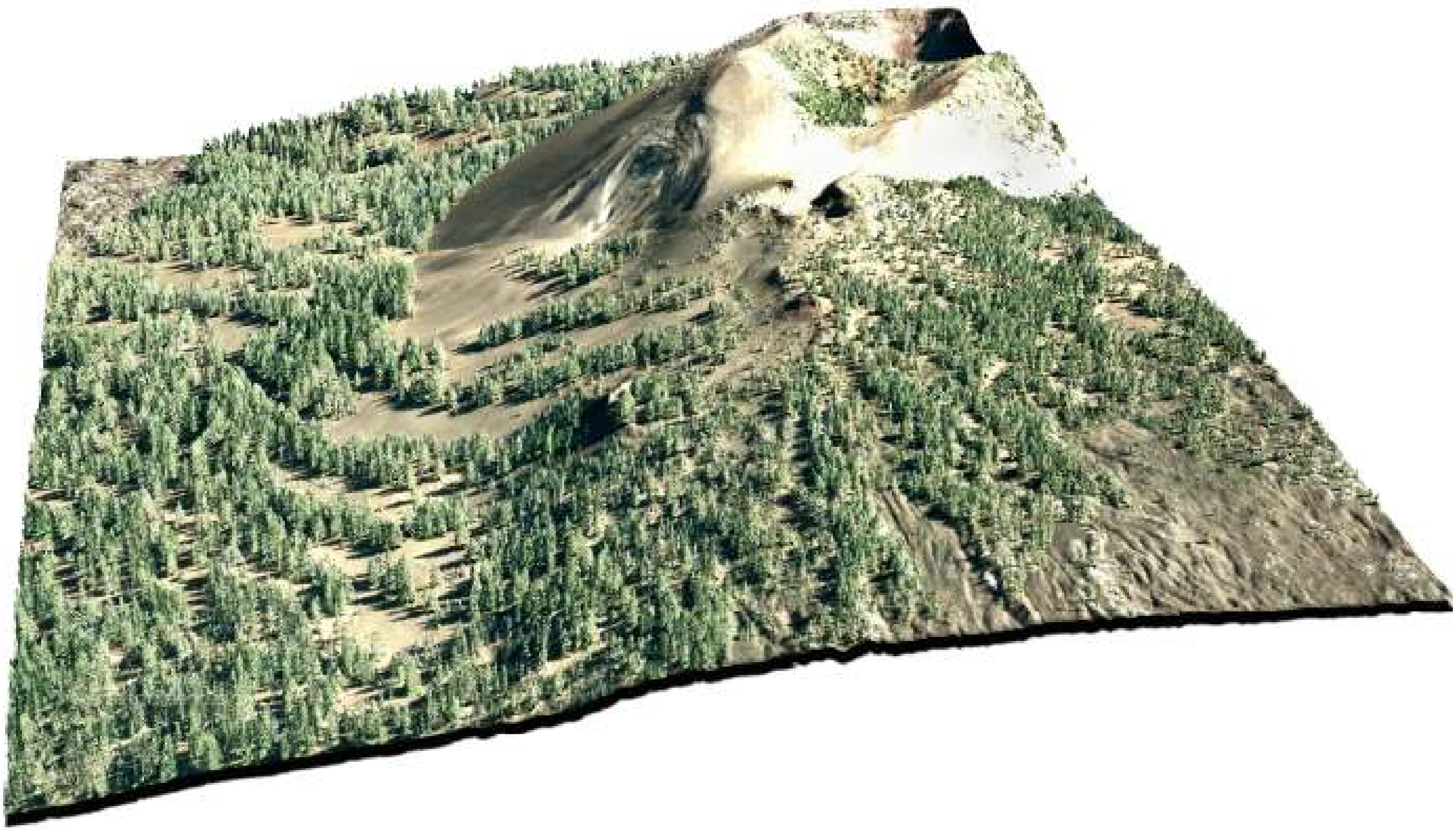

Figure 5.11. *Mt. Washington viewed from the north. Image created from LiDAR point cloud with RGB values extracted from NAIP orthophoto.*

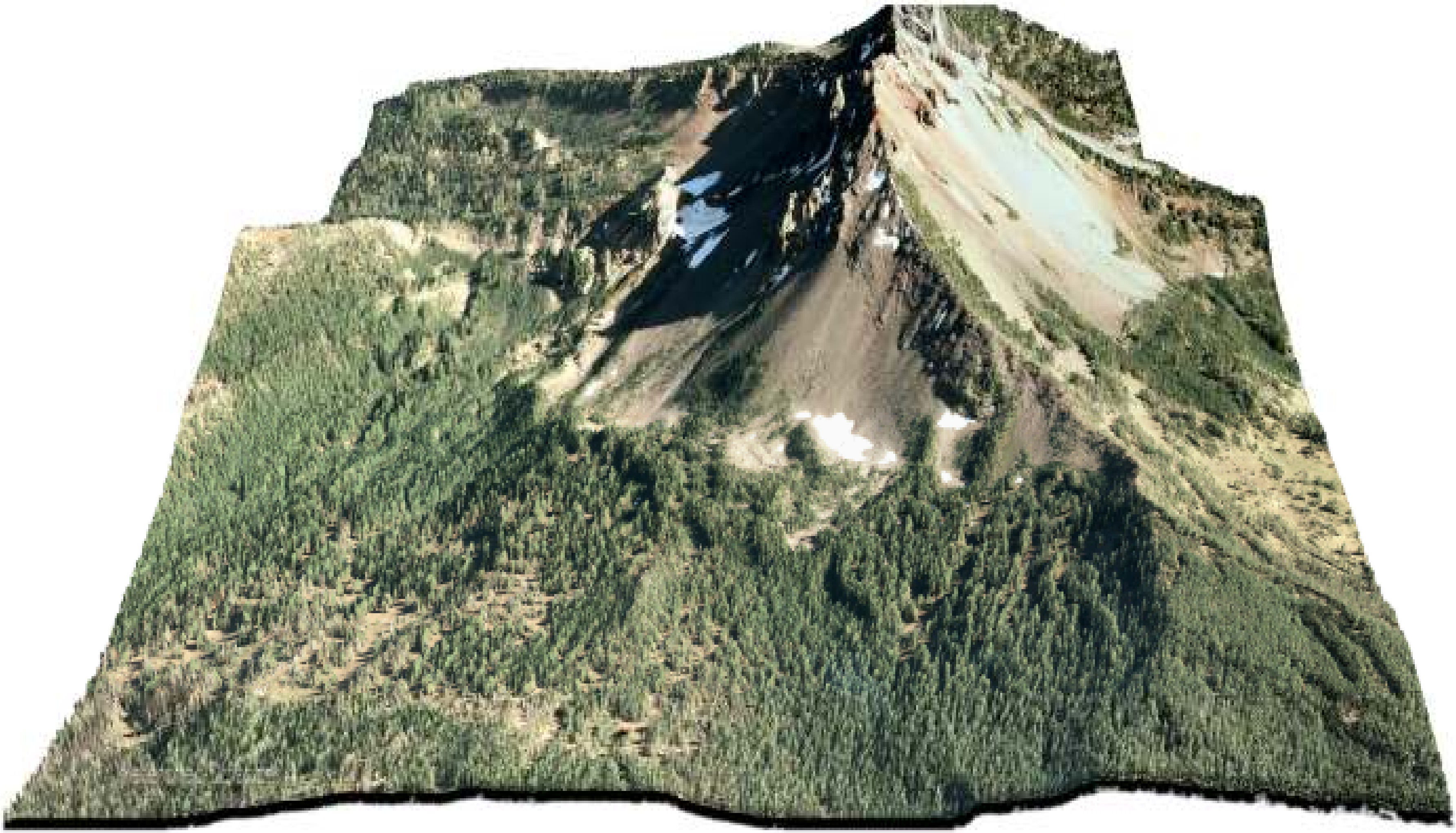

Figure 5.12. *The Crooked River below the Bowman Dam and Prineville Reservoir, OR. Image created from LiDAR point cloud with RGB values extracted from NAIP orthophoto.*

Figure 5.13. *The Crooked River south of Prineville, OR. Image created from LiDAR point cloud with RGB values extracted from NAIP orthophoto.*

Figure 5.14. *Gopher Gulch Airstrip, south of Tumalo State Park, OR. Image created from LiDAR point cloud with RGB values extracted from NAIP orthophoto.*

***Figure 5.15**. Riverview Park Golf Course and Highway 97 along the Deschutes River, North of Bend, OR. Image created from LiDAR point cloud with RGB values extracted from NAIP orthophoto.*

Figure 5.16. *Cliffs near Tumalo Falls, on Tumalo Creek. Image created with a three dimensional LiDAR point cloud with RGB values extracted from NAIP orthophotos.*

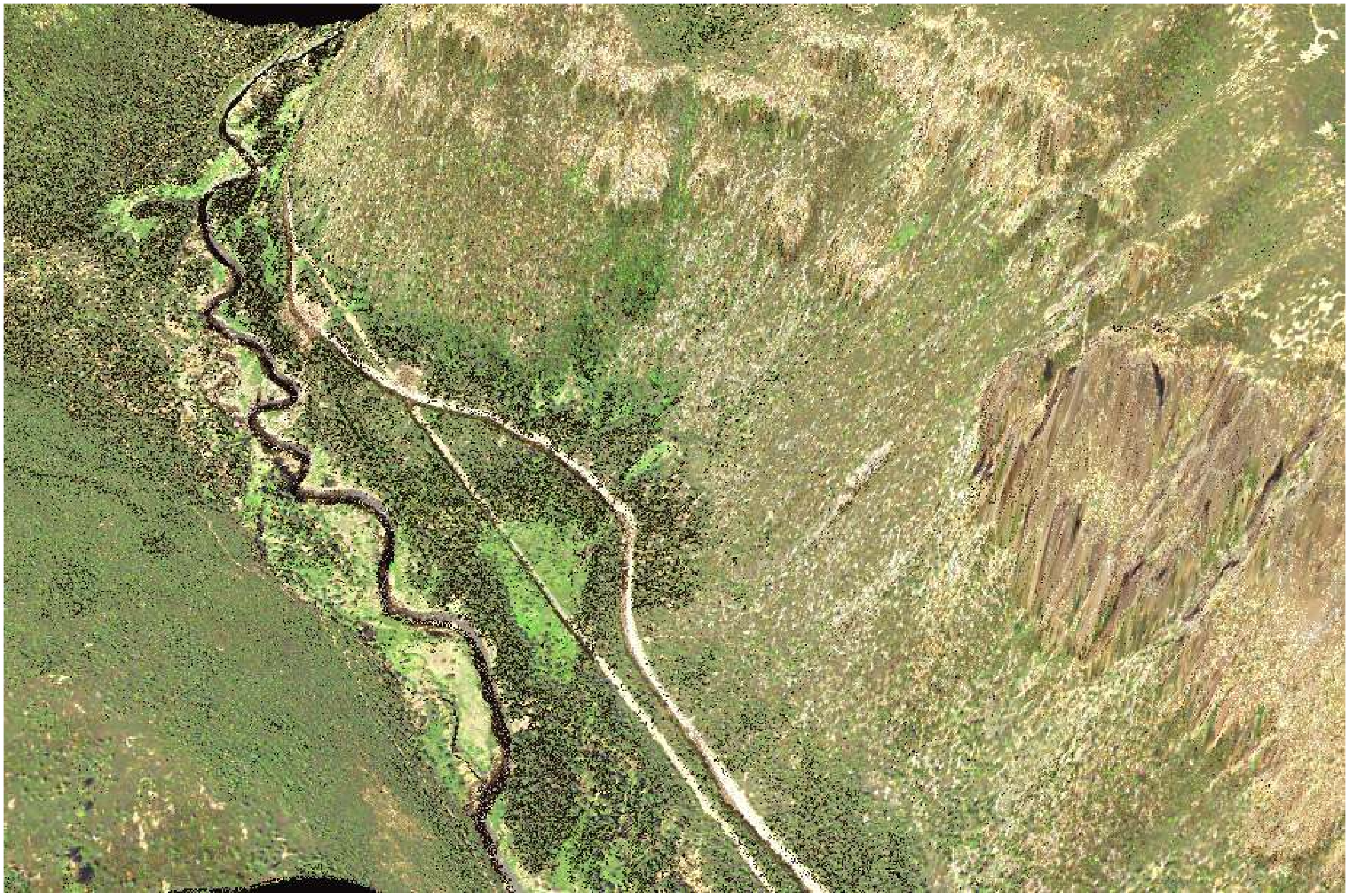

Figure 5.17. *Andesite volcano cone west of Sun River, Oregon. Image created with a three dimensional LiDAR point cloud with RGB values extracted from NAIP orthophotos.*

Figure 5.18. *Ski hill on Willamette Pass. Image created with a three dimensional LiDAR point cloud with RGB values extracted from NAIP orthophotos.*

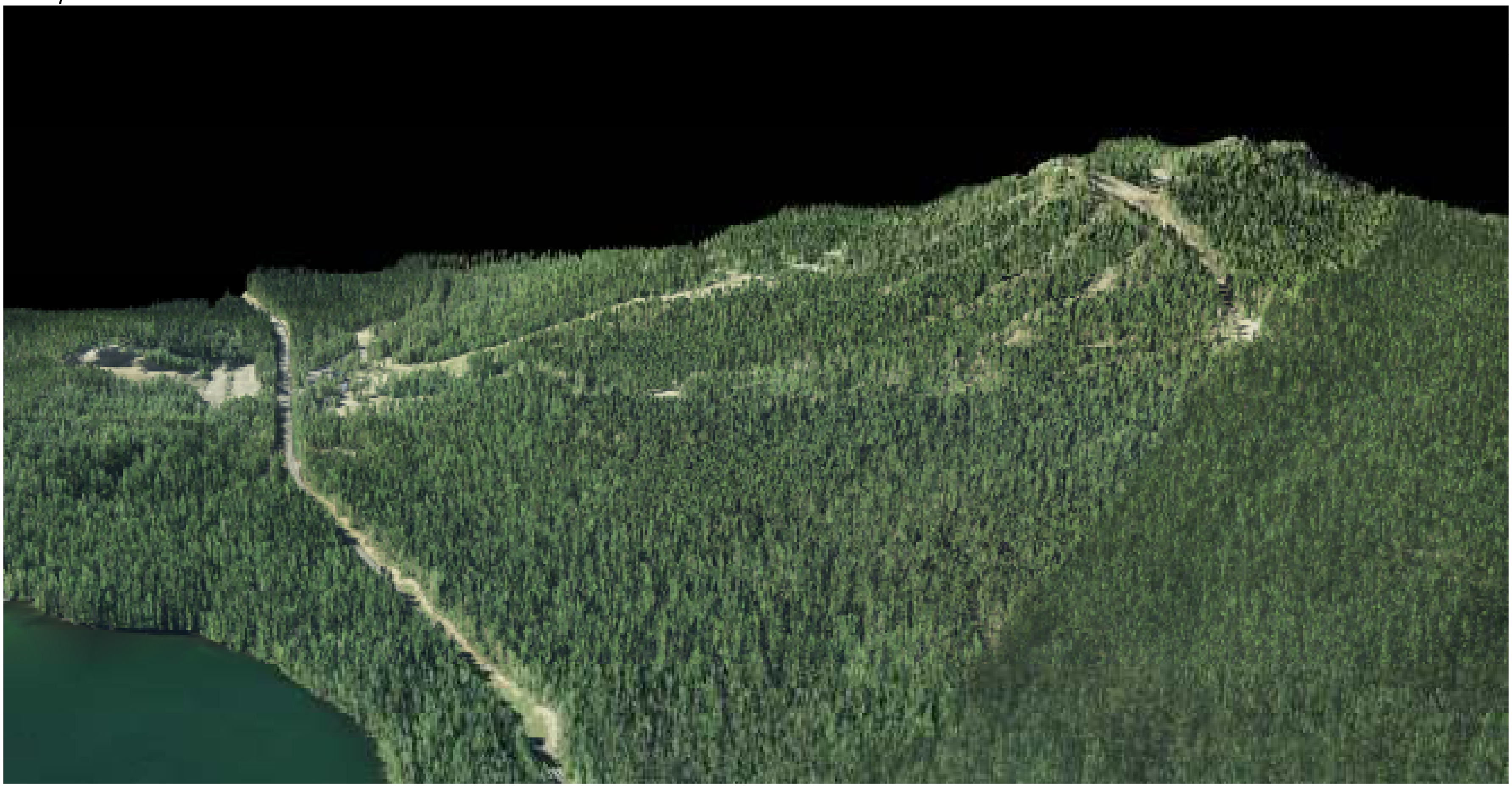

***Figure 5.19**. Lava Flow along Crescent Cutoff Road, OR. View is from the Northeast. Image created with a three dimensional LiDAR point cloud with RGB values extracted from NAIP orthophotos.*

Figure 5.20. *Odell Butte is a shield Volcano and the lava flow occurred 4740 years ago. It is near David Lake in Deschutes National Forest. Image created with a three dimensional LiDAR point cloud with RGB values extracted from NAIP orthophotos.*